Probing Nuclear Symmetry Energy

Bao-An Li

Physics & Astronomy
Texas A&M University-Commerce

Some random thoughts on:

- What do we currently know about $E_{sym}(\rho)$? (no consensus, my biased opinion)
- Why is the $E_{sym}(\rho)$ still so uncertain especially at high densities?
- What is the composition of $E_{sym}(\rho)$?
- What is the most fundamental but least known physics underlying $E_{sym}(\rho)$?

An example:

probing neutron skin and $E_{sym}(\rho)$ with intermediate E heavy-ion collisions

DESC0013702,

DE-SC0009971 (CUSTIPEN)

Office of Science
U.S. DEPARTMENT OF ENERGY

A White Paper for the 2023 US Nuclear Physics Long Range Plan

Dense Nuclear Matter Equation of State from Heavy-Ion Collisions

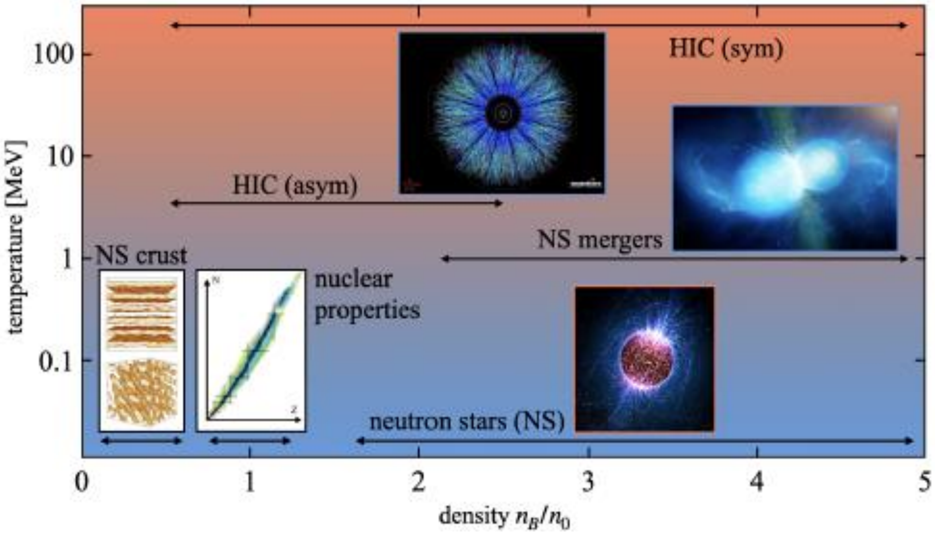

arXiv:2301.13253

Welcome your comments & suggestions
To become an endorsing author,
email to Dr. Agnieszka Sorensen @ INT
agnieszka.sorensen@gmail.com

Current list of authors:

Sorensen, Agnieszka ; Agarwal, Kshitij ; Brown, Kyle W. ; Chajecki, Zbigniew ; Danielewicz, Paweł ; Drischler, Christian ; Gandolfi, Stefano ; Holt, Jeremy W. ; Kaminski, Matthias ; Ko, Che-Ming ; Kumar, Rohit ; Li, Bao-An ; Lynch, William G. ; McIntosh, Alan B. ; Newton, William ; Pratt, Scott ; Savchuk, Oleh ; Stefaniak, Maria ; Tews, Ingo ; Tsang, ManYee Betty ; Vogt, Ramona ; Wolter, Hermann ; Zbroszczyk, Hanna ; Andronic, Anton ; Bass, Steffen A. ; Chbihi, Abdelouahad ; Colonna, Maria ; Cozma, Mircea Dan ; Dexheimer, Veronica ; Dong, Xin ; Dore, Travis ; Du, Lipei ; Harris, Steven P. ; Huang, Huan Zhong ; Jiménez, José C. ; Kapusta, Joseph ; Le Fèvre, Arnaud ; McLerran, Larry ; Noronha-Hostler, Jacquelyn ; Plumberg, Christopher ; Randrup, Jørgen ; Reddy, Sanjay ; Schmidt, Hans-Rudolf ; Senger, Peter ; Seto, Richard ; Shen, Chun ; Steinheimer, Jan ; Stroth, Joachim ; Sturm, Christian ; Sun, Kai-Jia ; Trautmann, Wolfgang ; Verde, Giuseppe ; Vovchenko, Volodymyr ; Xu, Nu

Empirical parabolic law of the EOS of cold, neutron-rich nucleonic matter

symmetry energy

Isospin asymmetry

$$E(\rho_n,\rho_p)=E_0(\rho_n=\rho_p)+E_{sym}(\rho)\left(\frac{\rho_n-\rho_p}{\rho}\right)^2+o(\delta^4)$$

Energy per nucleon in symmetric matter

Energy in asymmetric nucleonic matter

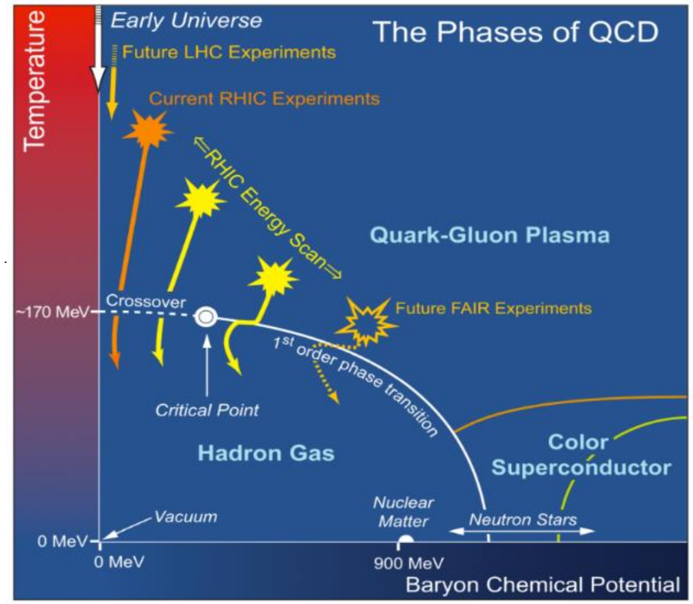

density

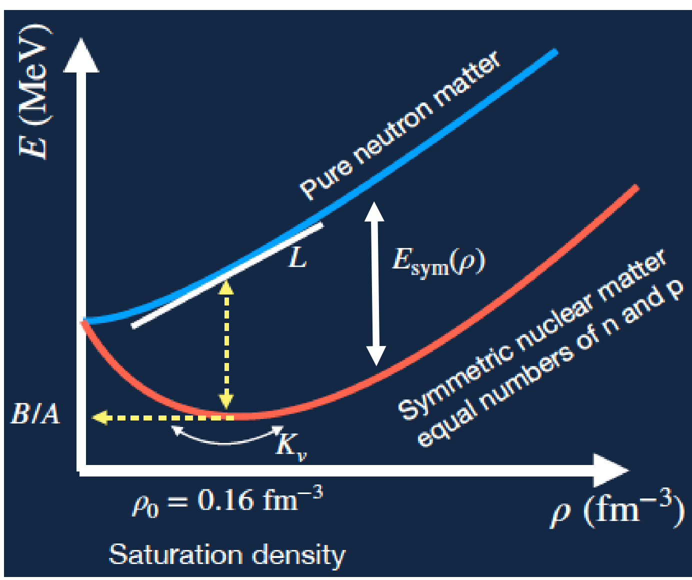

New opportunities

Isospin asymmetry

$\delta = (\rho_n - \rho_p)/\rho$

Isospin effects in observables of structures & collisions of neutron stars & heavy nuclei

$P_{asy}(\rho)$

$$E_{\rm sym}(\rho)=E_{\rm sym}(\rho_i)+\int_{\rho_i}^{\rho}\frac{P_{\rm PNM}(\rho_v)-P_{\rm SNM}(\rho_v)}{\rho_v^2}d\rho_v$$

Fundamental Microphysics Theories underlying each term in the EOS , what …, why …., where …how

Experimental and Observational Macrophysics underlying each observable and phenomenon, what …, why …., where …how

Empirical parameterizations especially useful for meta-modeling of EOS

Transport model simulations of heavy-ion collisions, energy density functionals for nuclear structures, Bayesian inferences of EOS, properties of neutron stars, waveforms of gravitational waves, ….

$$E(\rho,\delta) = E_0(\rho) + E_{\rm sym}(\rho)\cdot\delta^2$$

Assuming no hadron-quark phase transition

$$E_0(\rho) = E_0(\rho_0) + \frac{K_0}{2}\left(\frac{\rho-\rho_0}{3\rho_0}\right)^2 + \frac{J_0}{6}\left(\frac{\rho-\rho_0}{3\rho_0}\right)^3 + \frac{Z_0}{24}\left(\frac{\rho-\rho_0}{3\rho_0}\right)^4,$$

$$E_{\rm sym}(\rho) = E_{\rm sym}(\rho_0) + \frac{L}{3}\left(\frac{\rho}{\rho_0}-1\right) + \frac{K_{\rm sym}}{18}\left(\frac{\rho}{\rho_0}-1\right)^2 + \frac{J_{\rm sym}}{162}\left(\frac{\rho}{\rho_0}-1\right)^3 + \mathcal{O}\left[\left(\frac{\rho}{\rho_0}-1\right)^4\right]$$

Near the saturation density $\boldsymbol{\rho}_0$, they are Taylor expansions, appropriate for structure studies.
Just parameterizations when applied to heavy-ion collisions and the core of neutron stars

"Current" status of the restricted EOS parameter space:

Low density: $K_0 = 240 \pm 20$, $E_{\rm sym}(\rho_0) = 31.7 \pm 3.2$ and $L = 58.7 \pm 28.1$ MeV
High density: $-400 \leq K_{\rm sym} \leq 100$, $-200 \leq J_{\rm sym} \leq 800$, and $-800 \leq J_0 \leq 400$ MeV

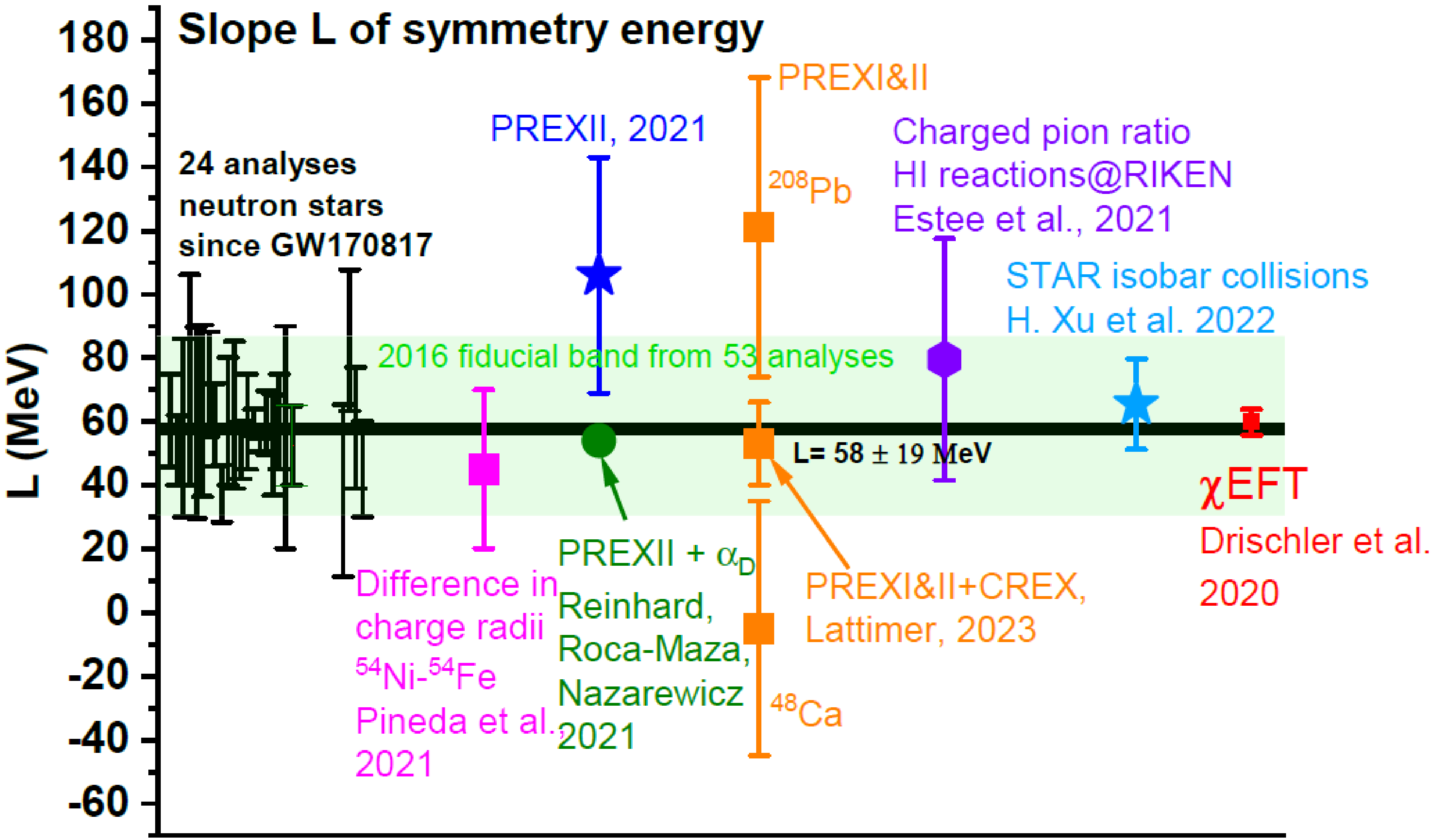
Slope L of symmetry energy
L (MeV)
180
160
140
120
100
80
60
40
20
0
-20
-40
-60
24 analyses
neutron stars
since GW170817
PREXII, 2021
PREXI&II
208Pb
48Ca
Charged pion ratio
HI reactions@RIKEN
Estee et al., 2021
STAR isobar collisions
H. Xu et al. 2022
2016 fiducial band from 53 analyses
L= 58 ± 19 MeV
χEFT
Drischler et al.
2020
Difference in
charge radii
54Ni-54Fe
Pineda et al.,
2021
PREXII + αD
Reinhard,
Roca-Maza,
Nazarewicz
2021
PREXI&II+CREX,
Lattimer, 2023

Curvature of the symmetry energy at saturation density

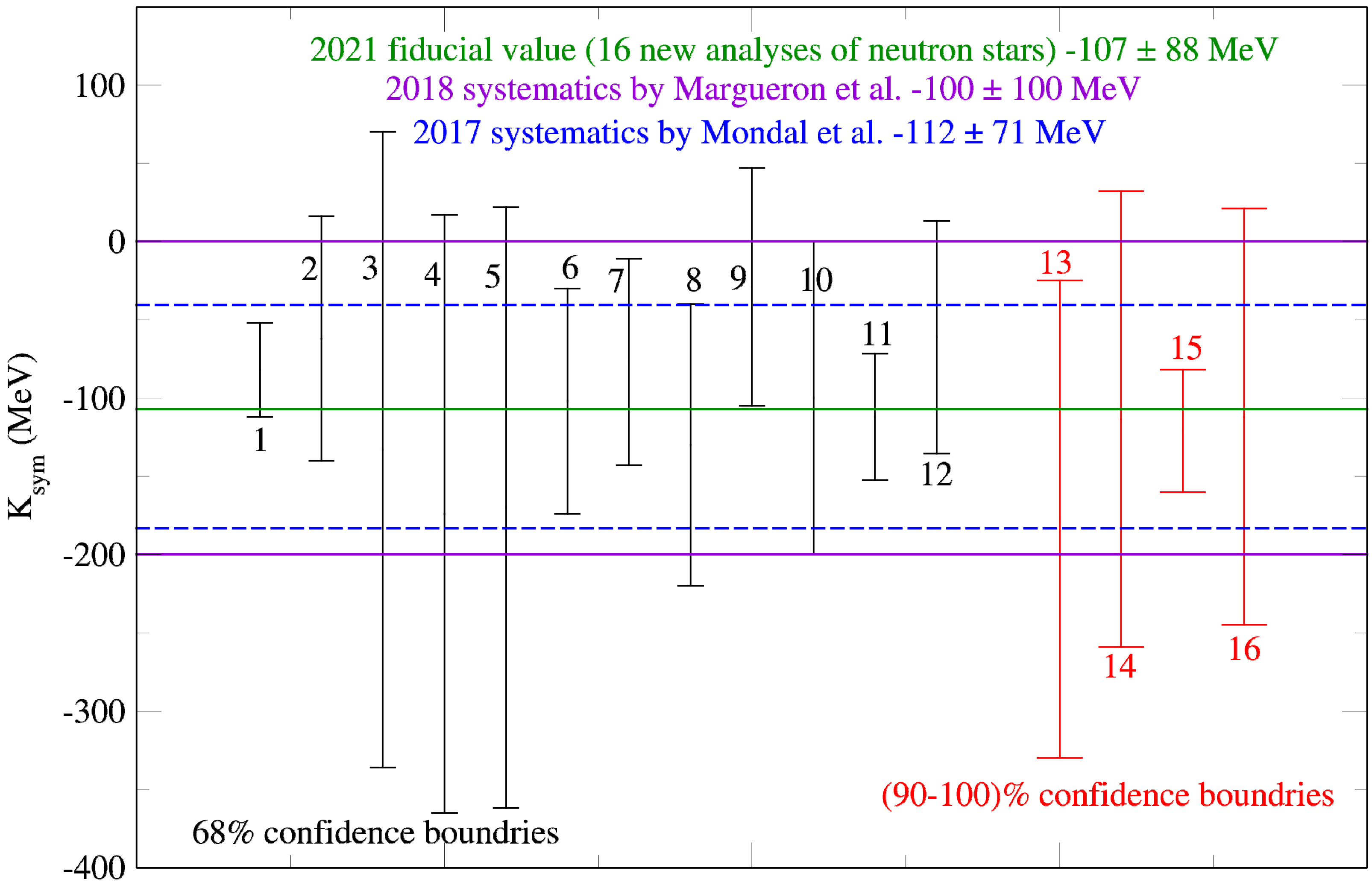

Currently available mass-radius observational data

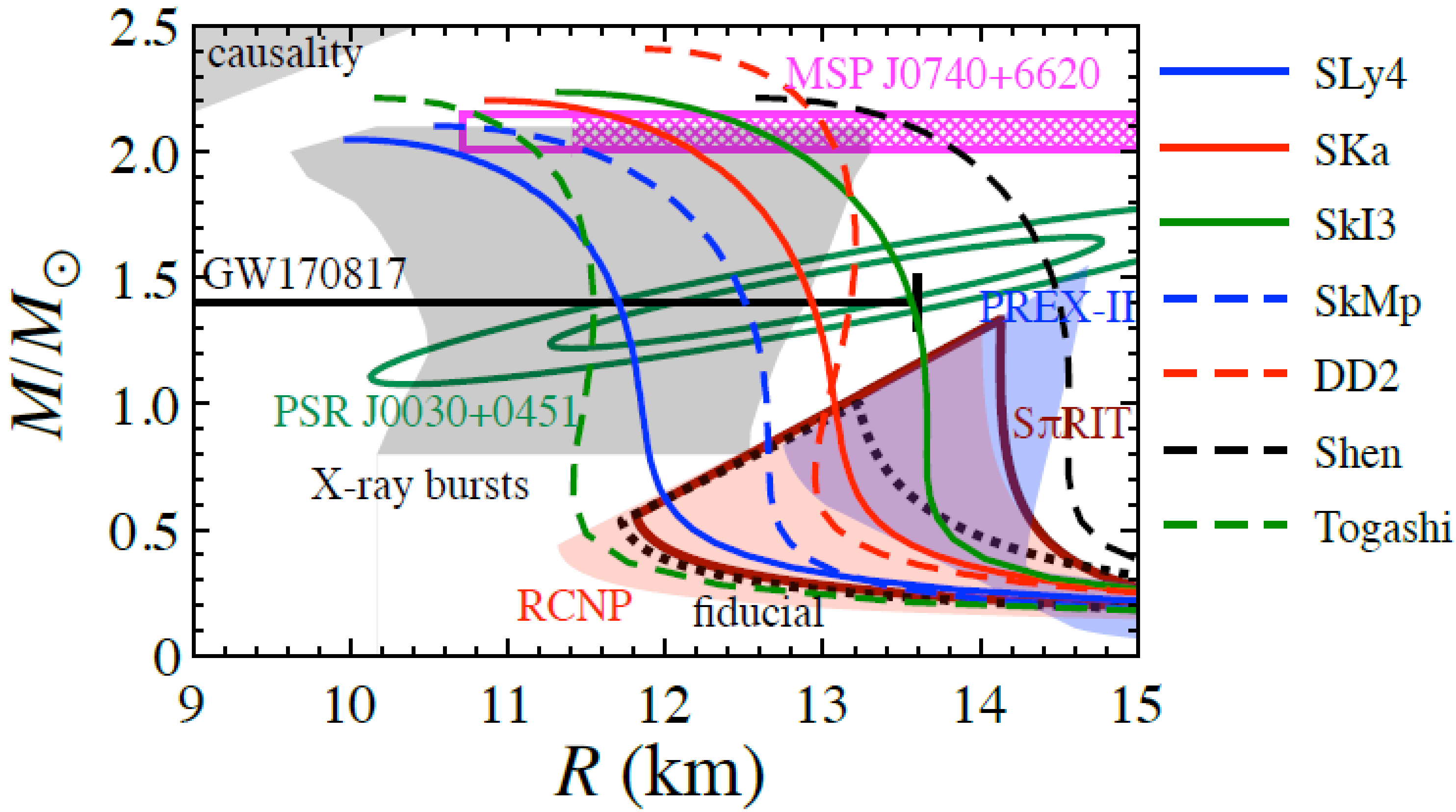

Hajime Sotani, Nobuya Nishimura, Tomoya Naito
Progress of Theoretical and Experimental Physics, Vol. 2022,
Issue 4, April 2022, 041D01, https://doi.org/10.1093/ptep/ptac055

Tidal deformability and radius from GW170817

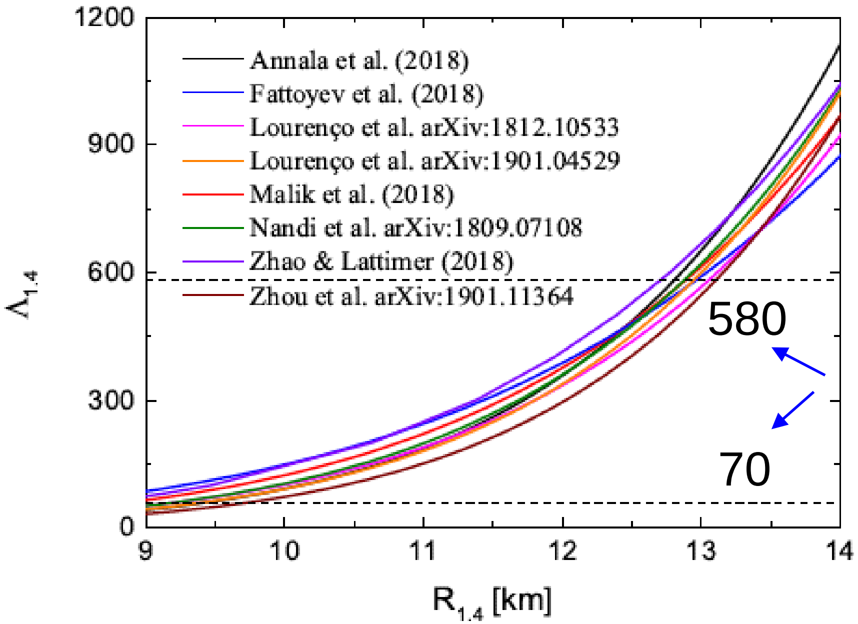

Directly from GW170817

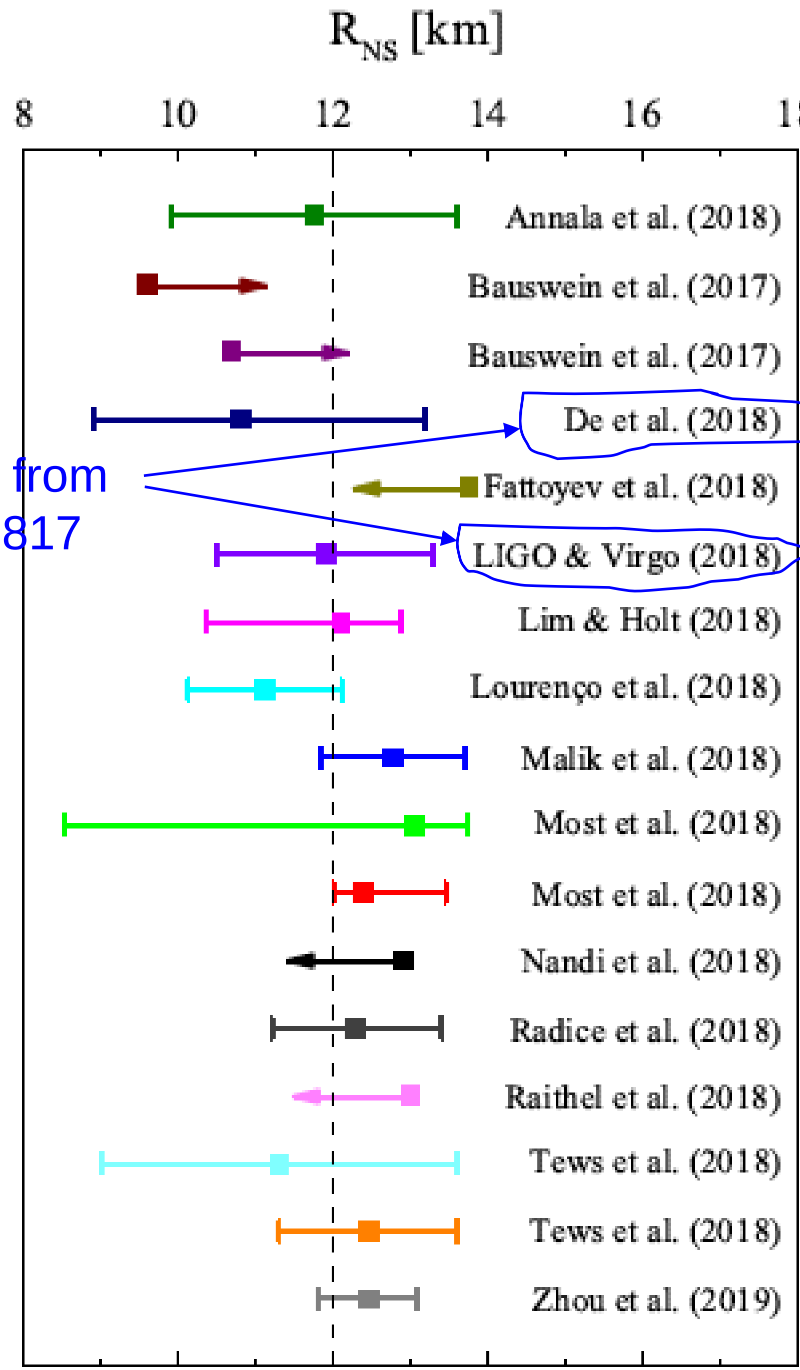

$$\Lambda = \frac{2}{3}\frac{k_2}{\beta^5}$$

B.A. Li, P.G. Krastev, D.H. Wen and N.B. Zhang
Review Article, EPJA 55, 117 (2019)

Wen-Jie Xie and Bao-An Li
APJ 883, 174 (2019)
APJ 899, 4 (2020)

Table 1. The radius $R_{1.4}$ data used in this work.

Radius $R_{1.4}$ (km) (90% confidence level)	Source	Reference
$11.9^{+1.4}_{-1.4}$	GW170817	(Abbott et al. 2018)
$10.8^{+2.1}_{-1.6}$	GW170817	(De et al. 2018)
$11.7^{+1.1}_{-1.1}$	QLMXBs	(Lattimer & Steiner 2014)
$11.9 \pm 0.8, 10.8 \pm 0.8, 11.7 \pm 0.8$	Imagined case-1	this work
11.9 ± 0.8	Imagined case-2	this work

Posterior probability distribution $P(\mathcal{M}|D) = \frac{P(D|\mathcal{M})P(\mathcal{M})}{\int P(D|\mathcal{M})P(\mathcal{M})d\mathcal{M}}$, **(Bayes' theorem)**

Likelihood: $P[D(R_{1,2,3})|\mathcal{M}(p_{1,2,\cdots 6})] = \prod_{j=1}^{3} \frac{1}{\sqrt{2\pi}\sigma_{\mathrm{obs},j}} \exp[-\frac{(R_{\mathrm{th},j} - R_{\mathrm{obs},j})^2}{2\sigma^2_{\mathrm{obs},j}}]$,

Meta-modeling of nuclear EOS

Uniform prior distribution P(M) in the ranges of

Table 2. Prior ranges of the six EOS parameters used

Parameters	Lower limit	Upper limit (MeV)
K_0	220	260
J_0	-800	400
K_{sym}	-400	100
J_{sym}	-200	800
L	30	90
$E_{\mathrm{sym}}(\rho_0)$	28.5	34.9

Bayesian inference of high-density E_{sym} from the radii $R_{1.4}$ of canonical neutron stars in 6D EOS parameter space

Posterior probability distribution function (PDF) of 6 EOS parameters from Bayesian analyses of GW170817 & NICER data for the canonical PSR J0030+0451 of masses around 1.4 solar mass

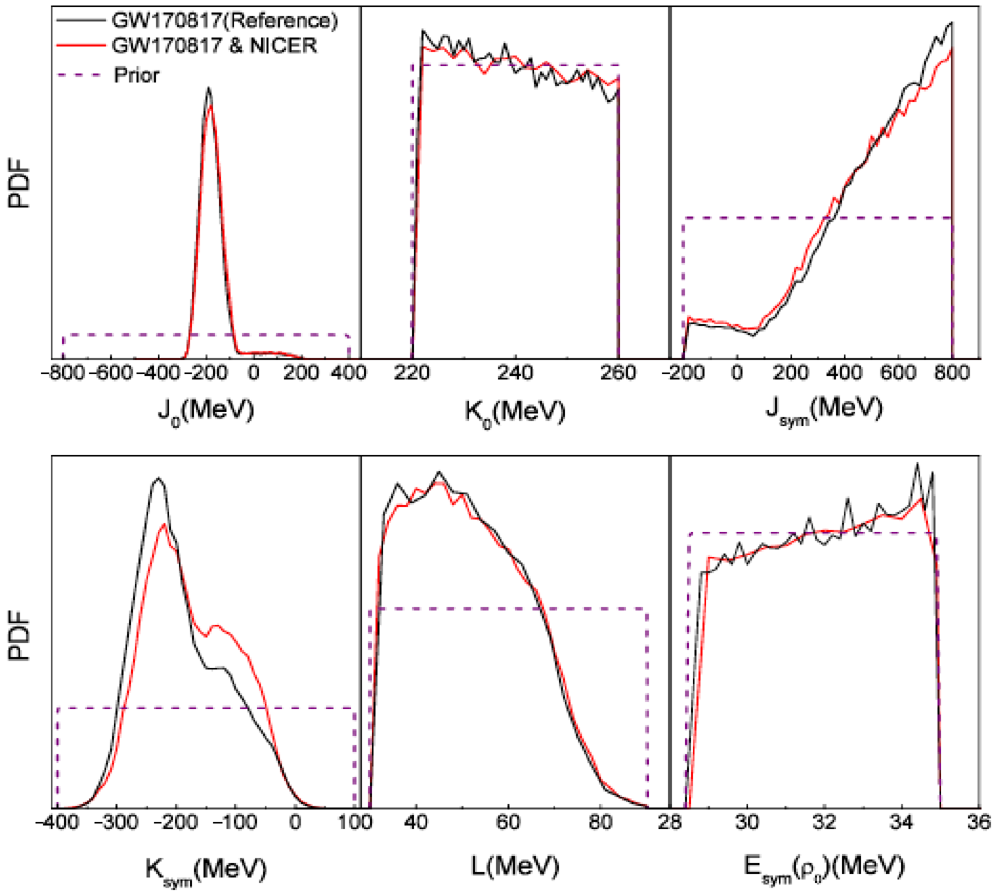

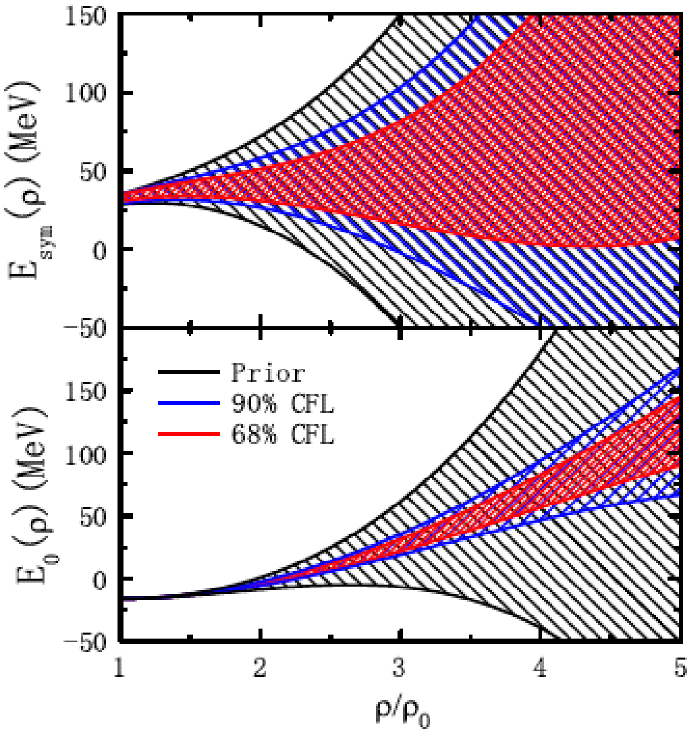

Wen-Jie Xie and Bao-An Li

APJ 883, 174 (2019)

APJ 899, 4 (2020)

Solving the NS inverse-structure problems by calling the TOV solver within 3 Do-Loops: Given an observable→ Find ALL necessary & sufficient EOSs

$$E_0(\rho) = E_0(\rho_0) + \frac{K_0}{2}\left(\frac{\rho-\rho_0}{3\rho_0}\right)^2 + \frac{J_0}{6}\left(\frac{\rho-\rho_0}{3\rho_0}\right)^3, \quad (2.15)$$

$$E_{sym}(\rho) = E_{sym}(\rho_0) + L\left(\frac{\rho-\rho_0}{3\rho_0}\right) + \frac{K_{sym}}{2}\left(\frac{\rho-\rho_0}{3\rho_0}\right)^2 + \frac{J_{sym}}{6}\left(\frac{\rho-\rho_0}{3\rho_0}\right)^3 \quad (2.16)$$

$$E(\rho,\delta) = E_0(\rho) + E_{sym}(\rho)\cdot\delta^2$$

Fix the saturation parameters $E_0(\rho_0)$, K_0, $E_{sym}(\rho_0)$ and L at their most probable values currently known

Example:

J_0=-189 is found given M_{max}=2.01M_{sun}

J_0 loop

Inversion by brute force

TOV

at K_{sym}=-200 & J_{sym}=400 inside the K_{sym} and J_{sym} loops

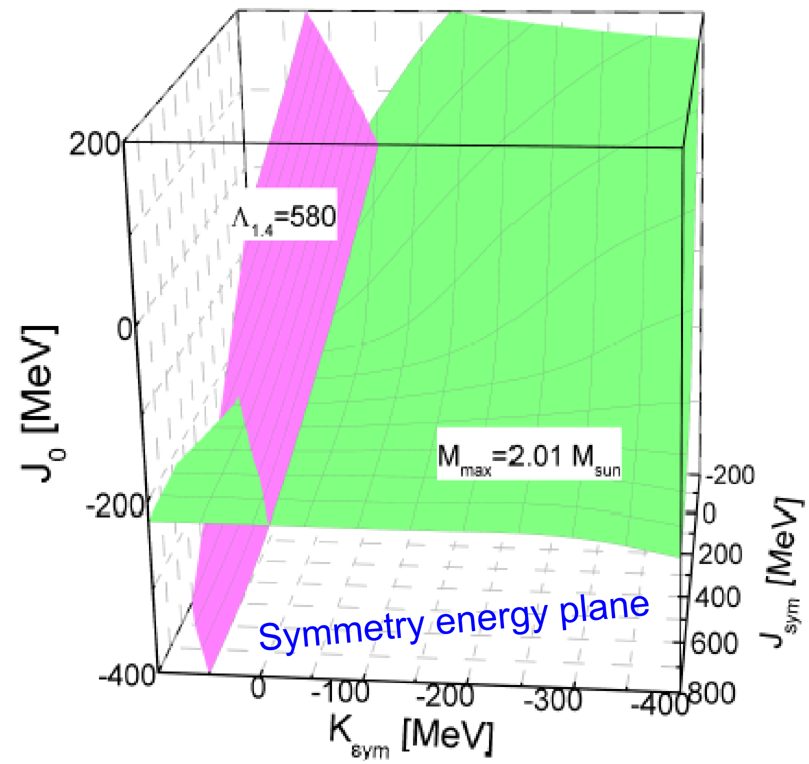

N.B. Zhang, B.A. Li and J. Xu, APJ 859, 90 (2018)

The Astrophysical Journal, 921:111 (11pp), 2021 November 10
https://doi.org/10.3847/1538-4357/ac1e8c

Impact of NICER's Radius Measurement of PSR J0740+6620 on Nuclear Symmetry Energy at Suprasaturation Densities

Nai-Bo Zhang[1] and Bao-An Li[2]

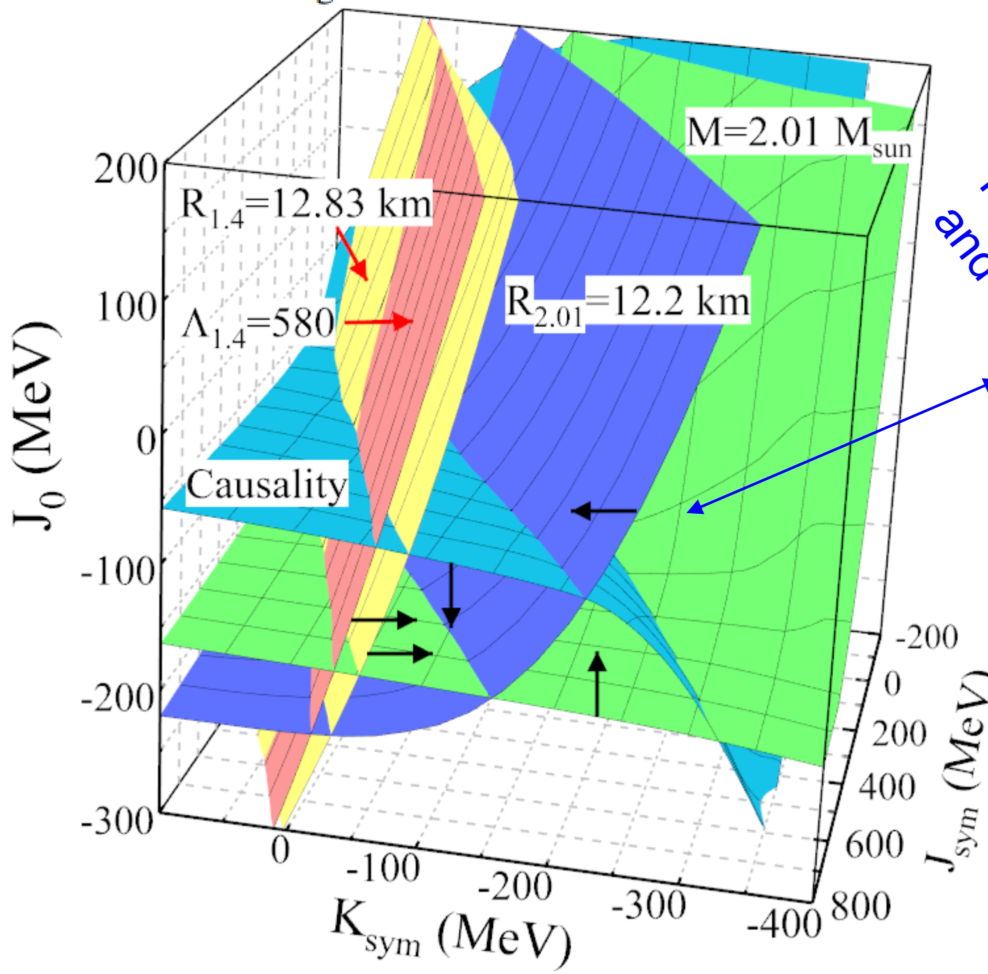

Power of simultaneous Measurements of mass and radius

NICER results :

Mass: $2.08 \pm 0.07\, M_{\odot}$

Radius: $13.7^{+2.6}_{-1.5}$ km (68%) (Miller et al. 2021) or $12.39^{+1.30}_{-0.98}$ km (Riley

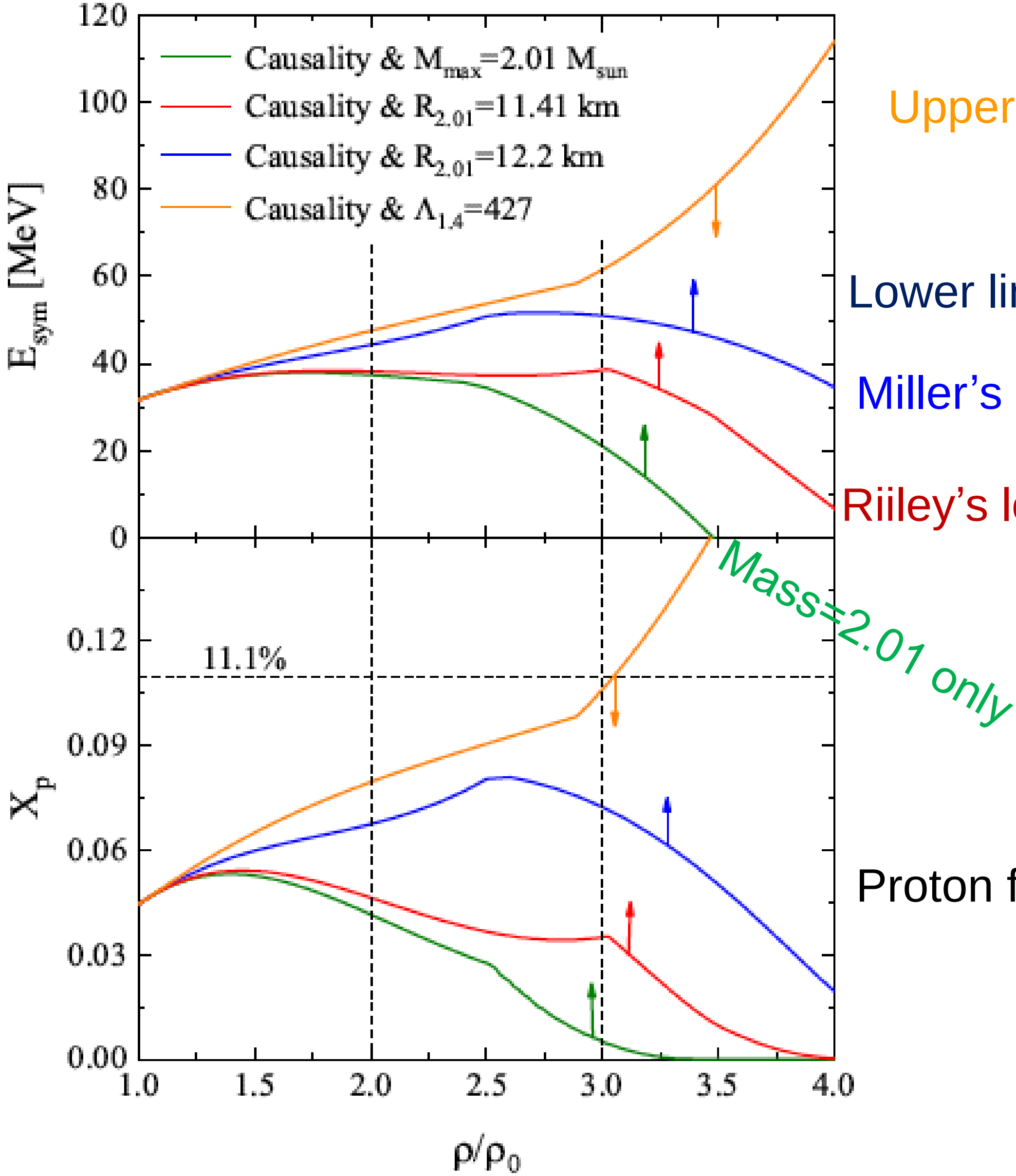

Upper limit on E_{sym} from GW170817

Lower limit on E_{sym} from PSR J0740+6620

Miller's lower radius

Riiley's lower radius

Proton fraction in PSR J0704+6620

N.B. Zhang and B.A Li
APJ 921, 111 (2021)

Why is the symmetry energy still so uncertain especially at high densities?

Phenomenological Models
60 examples

Microscopic & *ab initio* Theories
11 examples

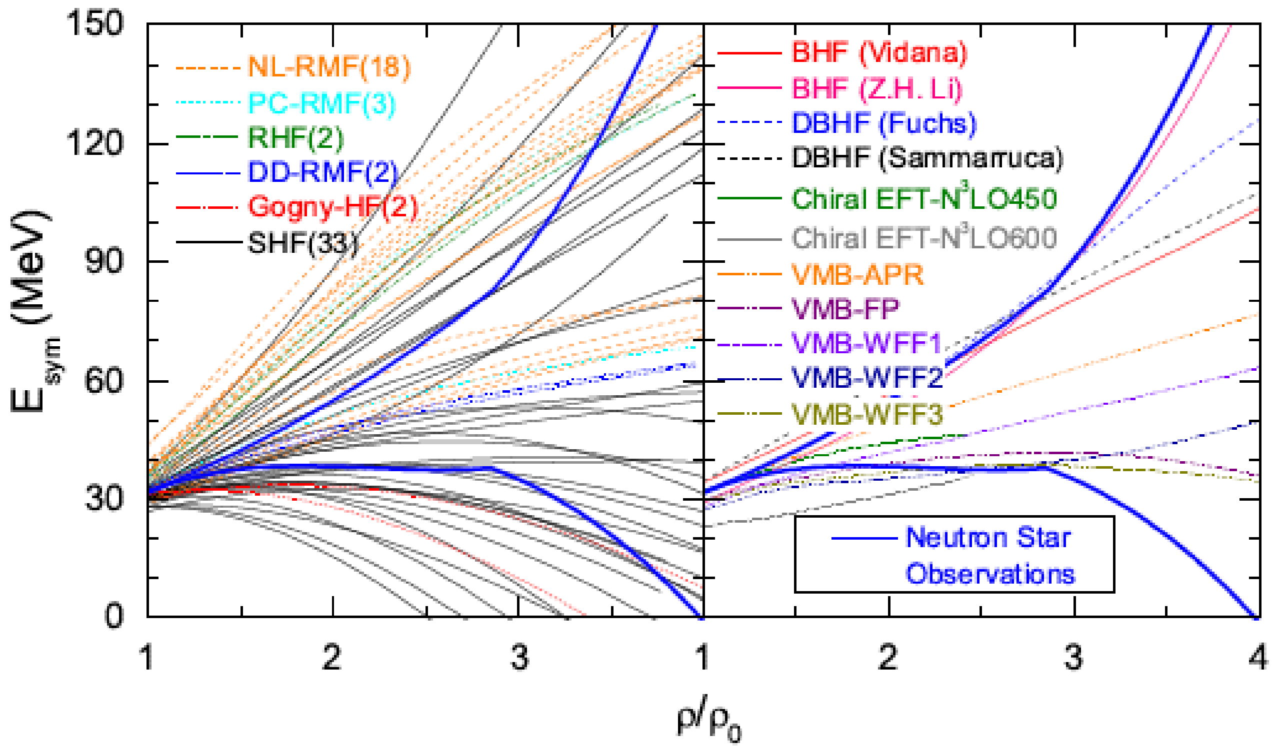

L.W. Chen, Nucl. Phys. Rev. 34, 20 (2017).
N.B. Zhang, B.A. Li, Eur. Phys. J. A 55, 39 (2019).

➢ E_{sym} around (1-2)ρ_0 is most relevant for determining the radii of canonical neutron stars, existing 1.4M_{sun}NS observations do NOT constrain much E_{sym} above 2ρ_0 where SRC effects are important.

Single-nucleon potential in isospin-asymmetric nuclear matter

+ for neutrons

$$U_{n/p}(k,\rho,\delta) = U_0(k,\rho) \pm U_{sym1}(k,\rho)\bullet\delta + U_{sym2}(k,\rho)\bullet\delta^2 + o(\delta^3)$$

- for protons

Isovector

According to the Hugenholtz-Van Hove (HVH) theorem: $E_F = \frac{d\xi}{d\rho} = \frac{d(\rho E)}{d\rho} = E + \rho\frac{dE}{d\rho} = E + P/\rho$

J. Dabrowski and P. Haensel, PLB 42, (1972) 163.

S. Fritsch, N. Kaiser and W. Weise, NPA. A750, 259 (2005).

C. Xu, B.A. Li, L.W. Chen, Phys. Rev. C 82 (2010) 054607.

$$E_{sym}(\rho) = \frac{1}{3}\frac{\hbar^2k^2}{2m_0^*}|_{k_F} + \frac{1}{2}U_{sym,1}(\rho,k_F),$$

Potential

$$L(\rho) = \frac{2}{3}\frac{\hbar^2k^2}{2m_0^*}|_{k_F} - \frac{1}{6}\left(\frac{\hbar^2k^3}{m_0^{*2}}\frac{\partial m_0^*}{\partial k}\right)|_{k_F} + \frac{3}{2}U_{sym,1}(\rho,k_F) + \frac{\partial U_{sym,1}}{\partial k}|_{k_F}\cdot k_F + 3U_{sym,2}(\rho,k_F),$$

Kinetic

Nucleon effective mass in isospin symmetric matter $m_0^*(\rho,k) = \frac{m}{1+\frac{m}{\hbar^2 k}\frac{\partial U_0(\rho,k)}{\partial k}},$

Neutron-proton effective mass splitting in neutron-rich matter

$$m_{n-p}^* \approx 2\delta\frac{m}{\hbar^2k_F}\left[-\frac{dU_{sym,1}}{dk} - \frac{k_F}{3}\frac{d^2U_0}{dk^2} + \frac{1}{3}\frac{dU_0}{dk}\right]_{k_F}\left(\frac{m_0^*}{m}\right)^2$$

$$\approx 2\delta\left(\frac{M_s^*}{M}\right)^2\left[\frac{M}{M_v^*} - \frac{M}{M_s^*}\right]$$

B.A. Li, B.J. Cai, L.W. Chen and J. Xu,
Progress of Particle and Nuclear Physics, 99 (2018) 29.

Density and momentum dependence of Isoscalar and Isovector potentials
Gogny Hartree-Fock predictions using 11 popular Gogny (finite-range) forces

PHYSICAL REVIEW C 90, 054327 (2014)

Isovector properties of the Gogny interaction

Roshan Sellahewa and Arnau Rios

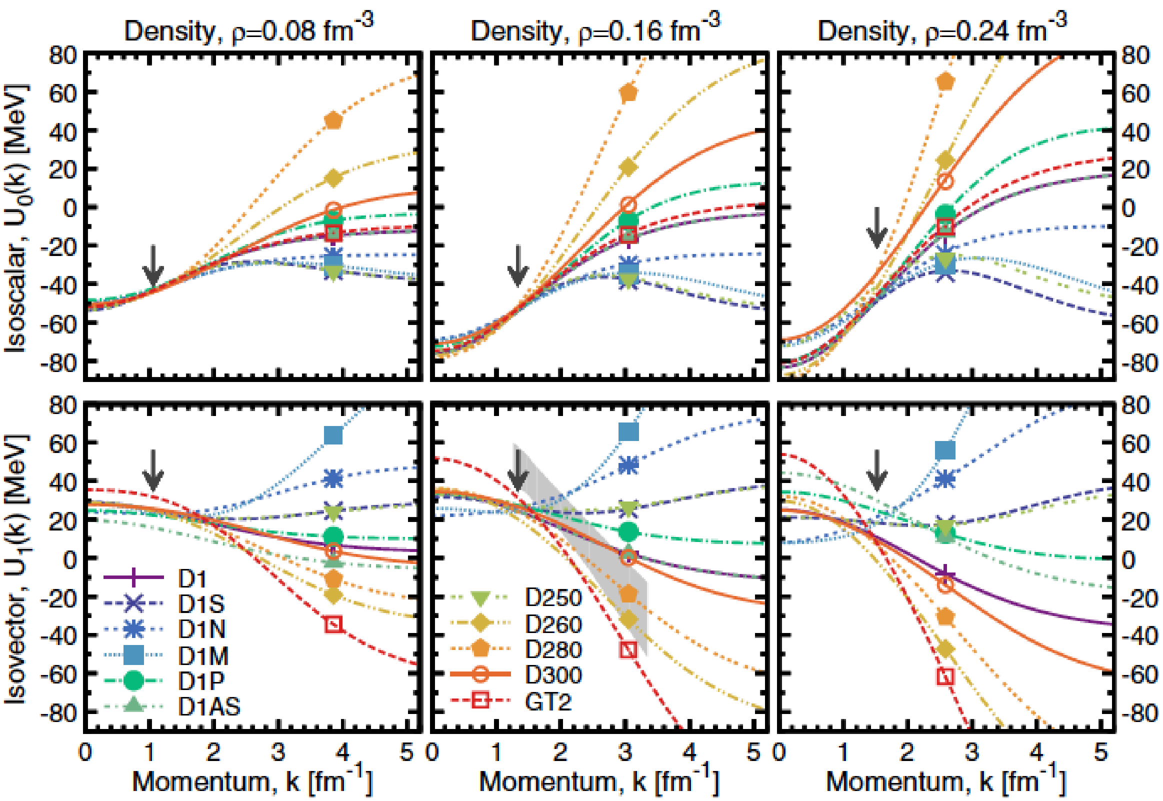

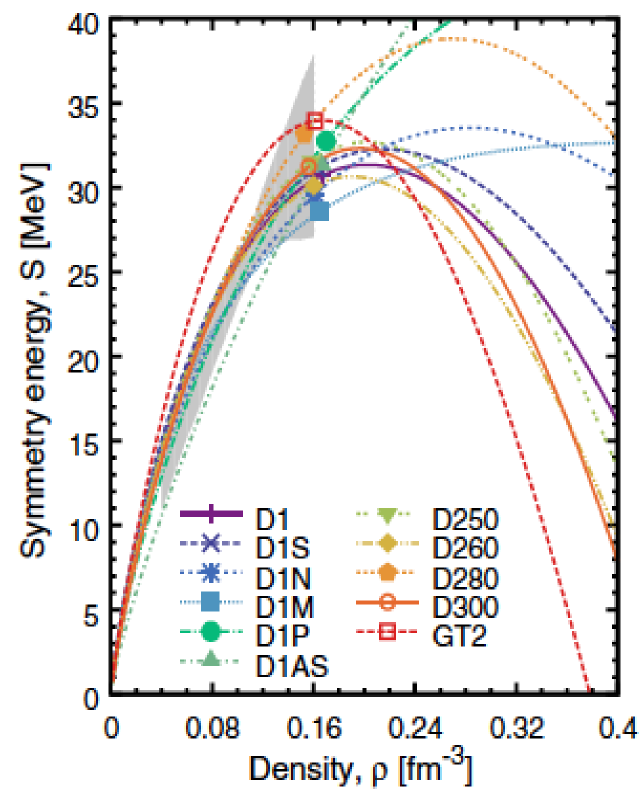

Symmetry potential at saturation density from global nucleon optical potentials

Systematics based on world data accumulated since 1969:

(1) Single particle energy levels from pick-up and stripping reaction
(2) Neutron and proton scattering on the same target at about the same energy
(3) Proton scattering on isotopes of the same element
(4) (p,n) charge exchange reactions

P.E. Hodgson, The Nucleon Optical Model, 1994 (World Scientific).

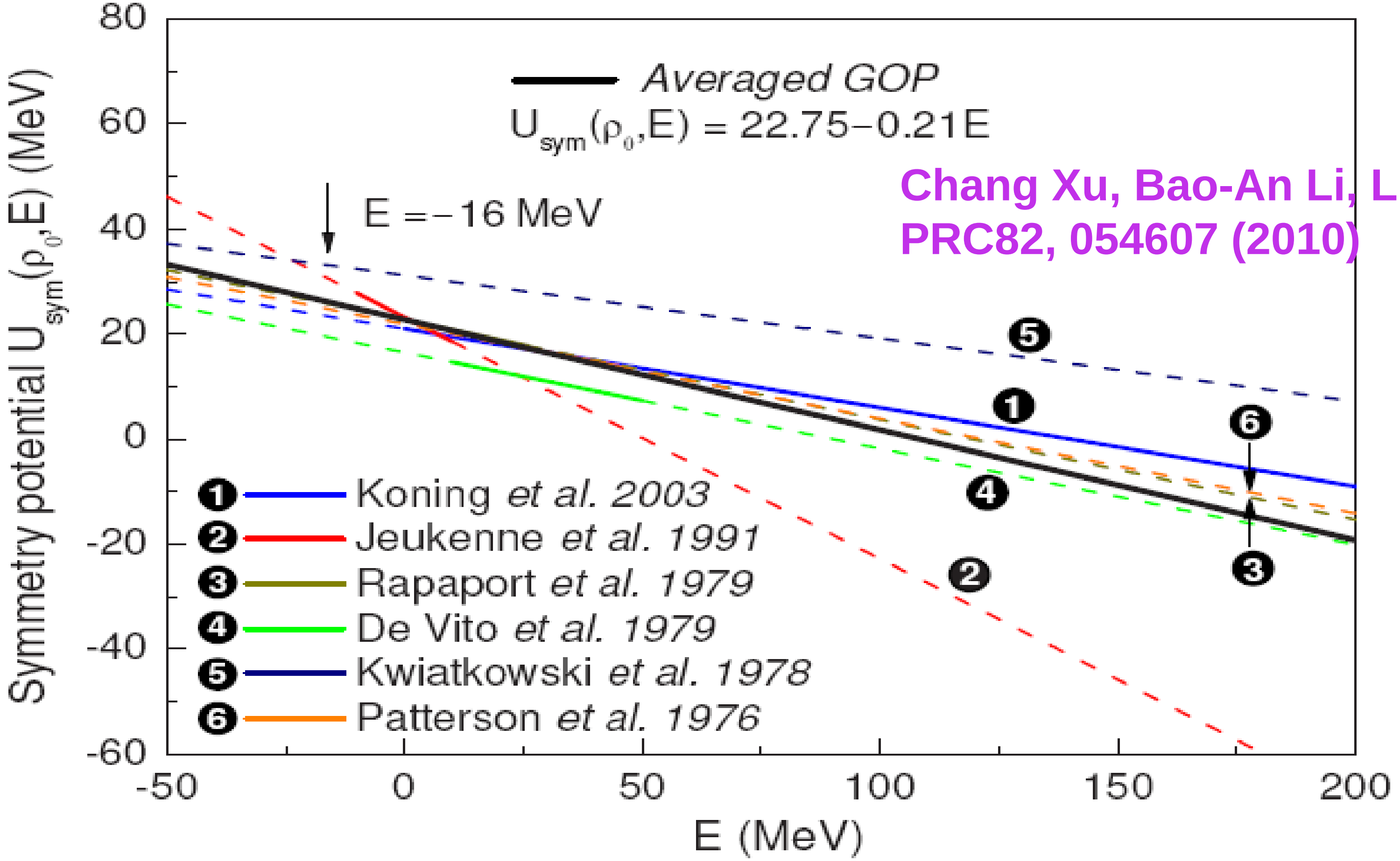

Chang Xu, Bao-An Li, Lie-Wen Chen, PRC82, 054607 (2010)

Momentum dependence of the nucleon optical potential at normal density

X.H. Li, W.J. Guo, B.A. Li, L.W. Chen, F.J. Fattoyev and W.G. Newton PLB 743 (2015) 408

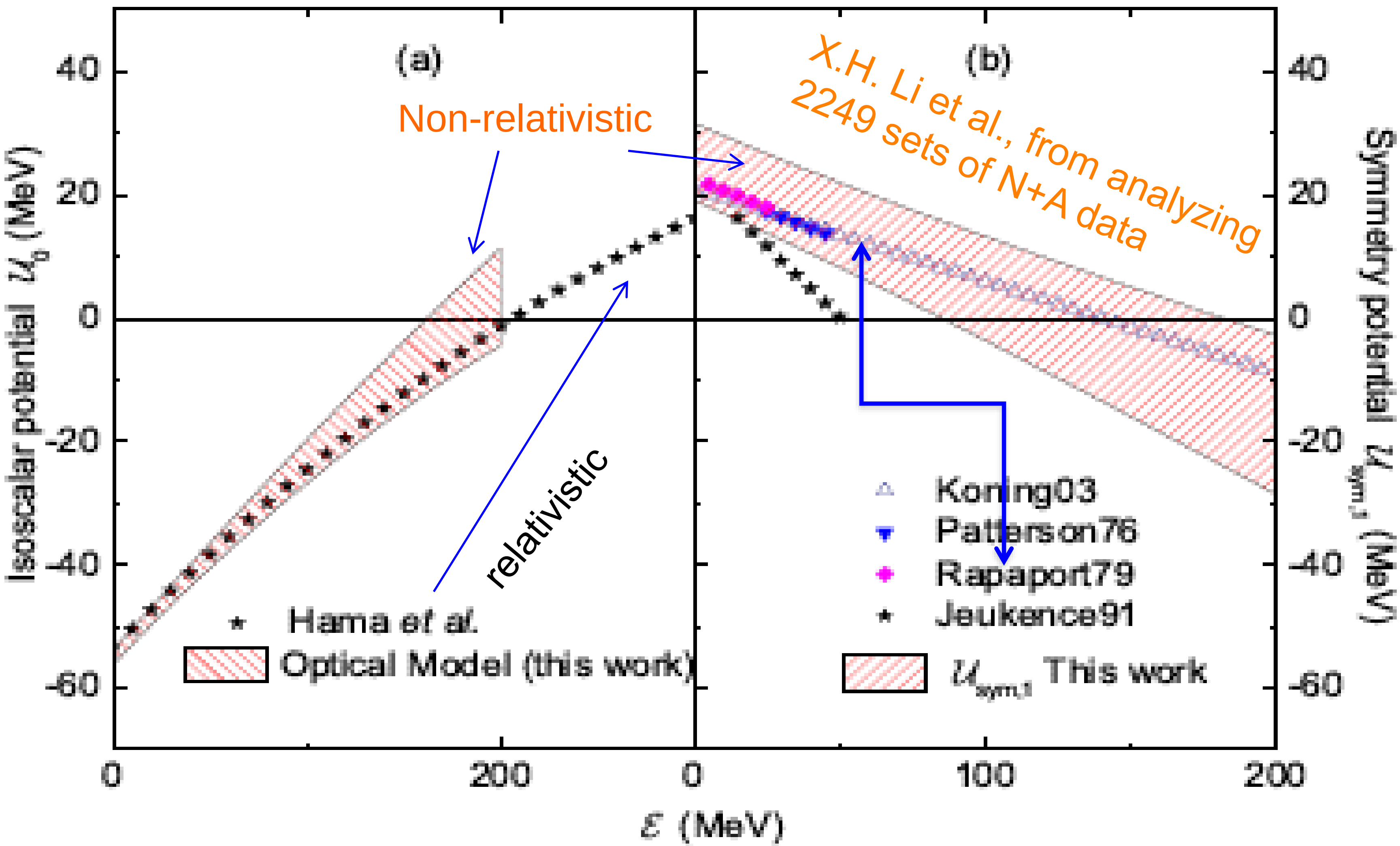

Constraining the symmetry energy and neutron-proton effective mass splitting using global nucleon optical potentials

Chang Xu, Bao-An Li, Lie-Wen Chen, PRC82, 054607 (2010)

$$E_{sym}(\rho) = \frac{1}{3}\frac{\hbar^2 k_F^2}{2m^*} + \frac{1}{2}U_{sym}(\rho, k_F)$$

$$E_{sym}(\rho_0) = 31.3 \text{ MeV} \pm 4.5 \text{ MeV}$$

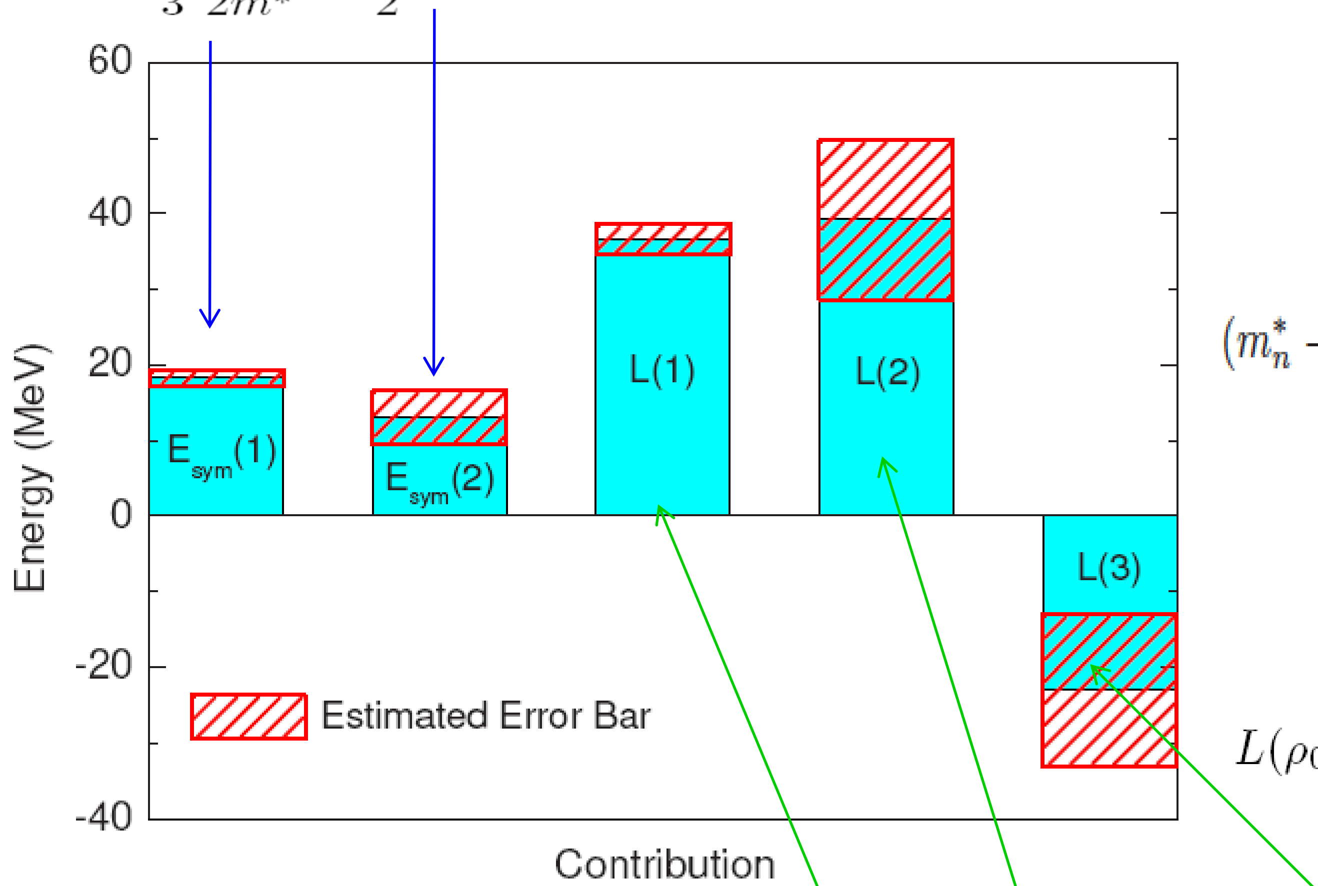

$$(m_n^* - m_p^*)/m = (0.32 \pm 0.15)\delta$$

$$L(\rho_0) = 52.7 \text{ MeV} \pm 22.5 \text{ MeV}$$

$$L(\rho) = \frac{2}{3}\frac{\hbar^2 k_F^2}{2m^*} + \frac{3}{2}U_{sym}(\rho, k_F) + \frac{\partial U_{sym}}{\partial k}|_{k_F} k_F$$

What are the fundamental physics behind the symmetry energy?

$$U_{n/p}(k,\rho,\delta) = U_0(k,\rho) \pm U_{sym1}(k,\rho)\bullet\delta + U_{sym2}(k,\rho)\bullet\delta^2 + o(\delta^3)$$

- **Isospin dependence of strong interactions and correlations**

$V_{T0} = V'_{np}$ (n-p pair in the T=0 state)

$V_{T1} = V_{nn} = V_{pp} = V_{np}$ (charge independence in the T=1 state)

Tensor force due to pion and **ρ** meson exchange MAINLY in the T=0 channel

$V_{np}(T0) \neq V_{np}(T1)$

In a simple interacting Fermi gas model:

Isospin-dependent correlation function

$$U_{sym}(k_F,\rho) = \frac{1}{4}\rho \int [V_{T1}(r_{ij}) f^{T1}(r_{ij}) - V_{T0}(r_{ij}) f^{T0}(r_{ij})] d^3 r_{ij}$$

Isospin-dependent effective 2-body interaction

M.A. Preston and R.K. Bhaduri, Structure of the Nucleus, 1975

Major issues relevant to high-density E_{sym}, heavy-ion reactions and neutron stars

- **Momentum dependence of the symmetry potential due to the finite-range of isovector int.**
- **Short-range correlations due to the tensor force in the isosinglet n-p channel**
- **Spin-isospin dependence of the 3-body force**
- **Isovector interactions of △(1232) resonances and their spectroscopy (mass and width)**
- **Possible sign inversion of the symmetry potential at high momenta/density**

Dominance of the isosinglet (T=0) interaction

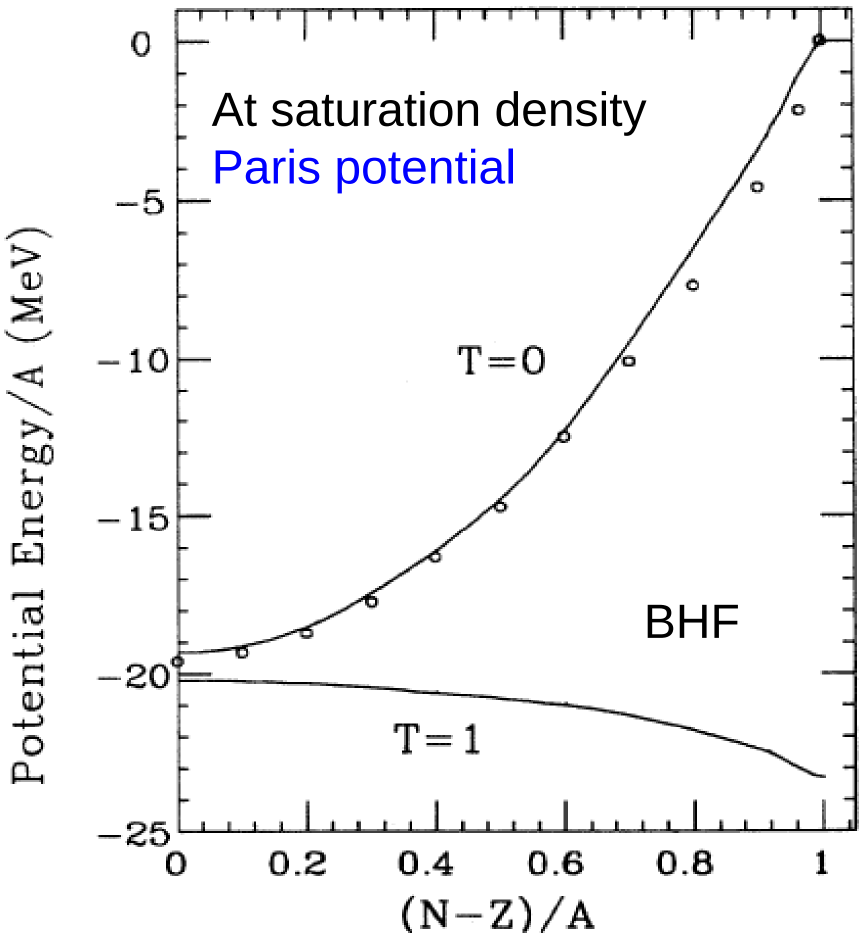

I. Bombaci and U. Lombardo PRC 44, 1892 (1991)

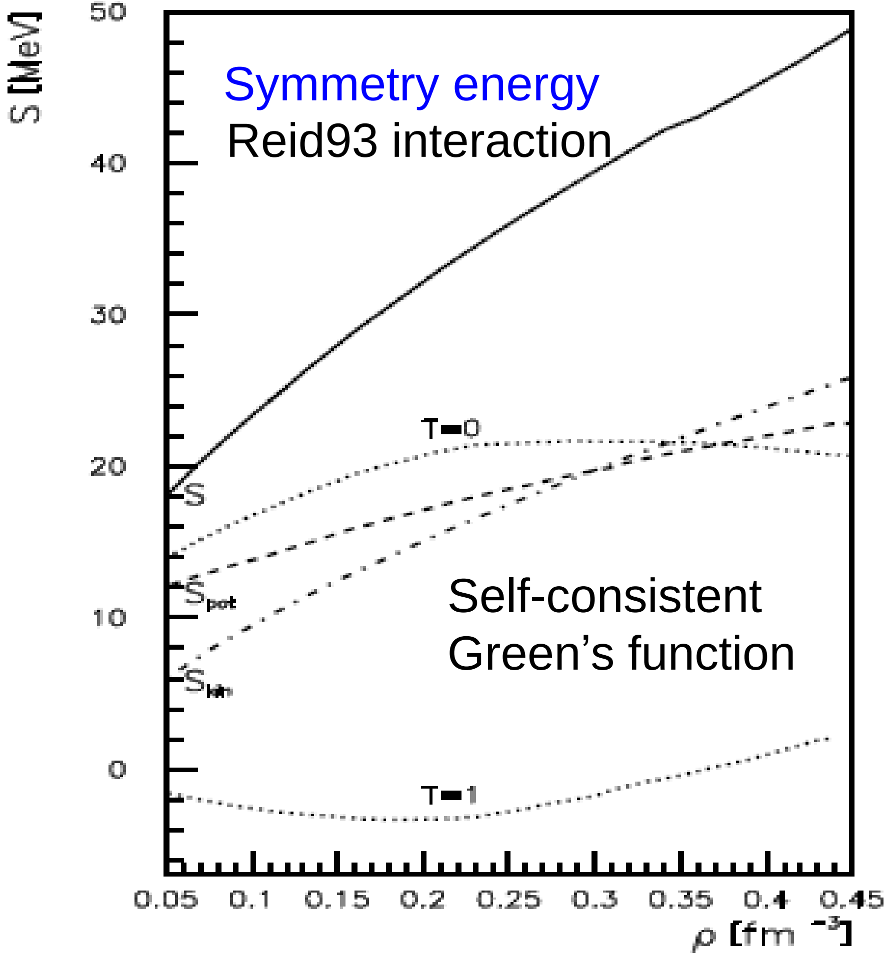

A.E.L. Dieperink,[1] Y. Dewulf,[2] D. Van Neck,[2] M. Waroquier,[2] and V. Rodin[3]

PRC68, 064307 (2003)

$$E_{sym}(\rho) = \frac{1}{2}\frac{\partial^2 E}{\partial \delta^2} \approx E(\rho)_{\text{pure neutron matter}} - E(\rho)_{\text{symmetric nuclear matter}}$$

The short and long range tensor force

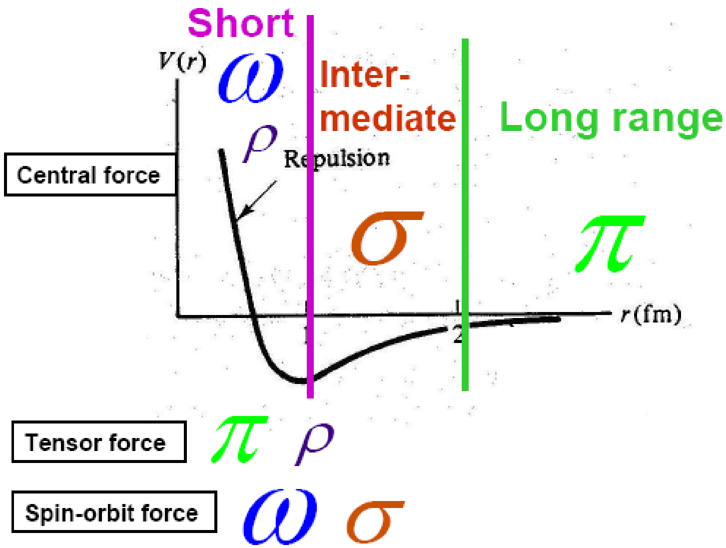

Lecture notes of R. Machleidt
CNS summer school, Univ. of Tokyo
Aug. 18-23, 2005

Strength of the tensor force

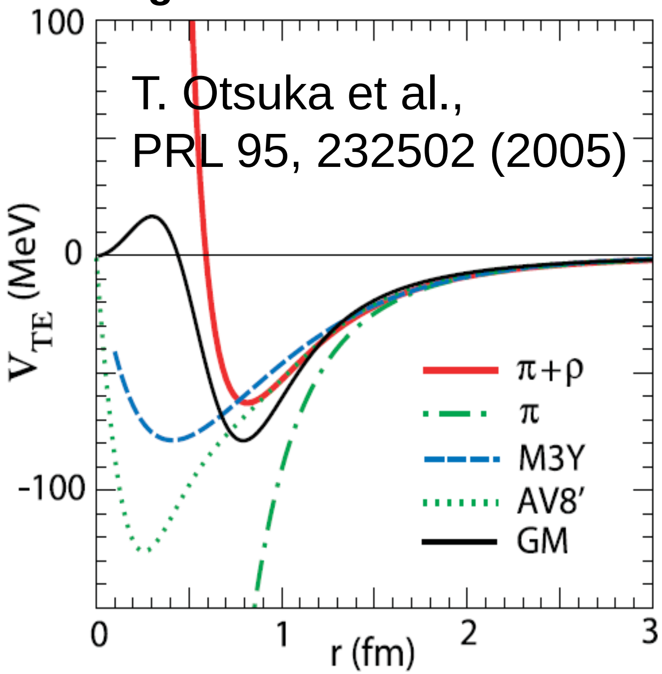

$\pi(138)$: $V_\pi = \frac{f_{\pi NN}^2}{3m_\pi^2}\frac{\vec{q}^2}{\vec{q}^2+m_\pi^2}[-\vec{\sigma}_1\cdot\vec{\sigma}_2 - S_{12}(\vec{q})]\vec{\tau}_1\cdot\vec{\tau}_2$ — Long-ranged tensor force

$\sigma(600)$: $V_\sigma \approx \frac{g_\sigma^2}{\vec{q}^2+m_\sigma^2}\left[-1-\frac{\vec{L}\cdot\vec{S}}{2M^2}\right]$ — intermediate-ranged, attractive central force plus LS force

$\omega(782)$: $V_\omega \approx \frac{g_\omega^2}{\vec{q}^2+m_\omega^2}\left[+1-3\frac{\vec{L}\cdot\vec{S}}{2M^2}\right]$ — short-ranged, repulsive central force plus strong LS force

$\rho(770)$: $V_\rho = \frac{f_\rho^2}{12M^2}\frac{\vec{q}^2}{\vec{q}^2+m_\rho^2}[-2\vec{\sigma}_1\cdot\vec{\sigma}_2 + S_{12}(\vec{q})]\vec{\tau}_1\cdot\vec{\tau}_2$ — short-ranged tensor force, opposite to pion

2^{nd} order tensor force contribution to the potential part of symmetry energy

G.E. Brown and R. Machleidt, Phys. Rev. C50, 1731 (1994).

S.-O. Bacnman, G.E. Brown and J.A. Niskanen, Phys. Rep. 124, 1 (1985).

T.T.S. Kuo and G.E. Brown, Phys. Lett. 18, 54 (1965)

$$< V_{\rm sym} > = \frac{12}{e_{\rm eff}} < [V_t(\mathbf{r})]^2 >$$

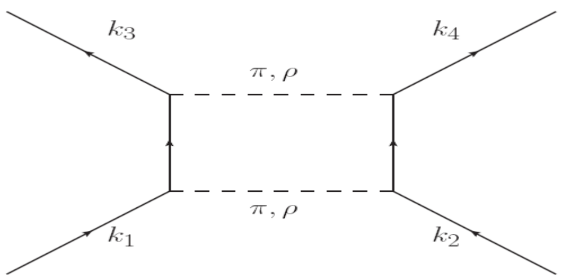

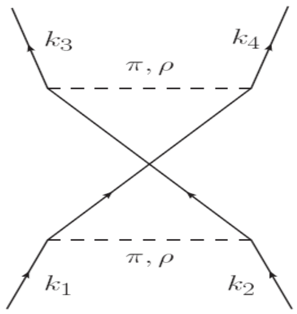

$$\frac{< V_{\rm sym} >}{A} = \frac{12}{e_{eff}} \cdot \frac{k_F^3}{12\pi^2} \{ \frac{1}{4} \int V_t^2(r) d^3r - \frac{1}{16} \int [\frac{3j_1(k_F r)}{k_F r}]^2 V_t^2(r) d^3r \}$$

Ang Li and Bao-An Li, arXiv:1107.0496

C. Xu, A. Li and B.A. Li, Journal of Physics: Conference Series 420, 012190 (2013)

Short-range tensor forces affects the high-density symmetry energy

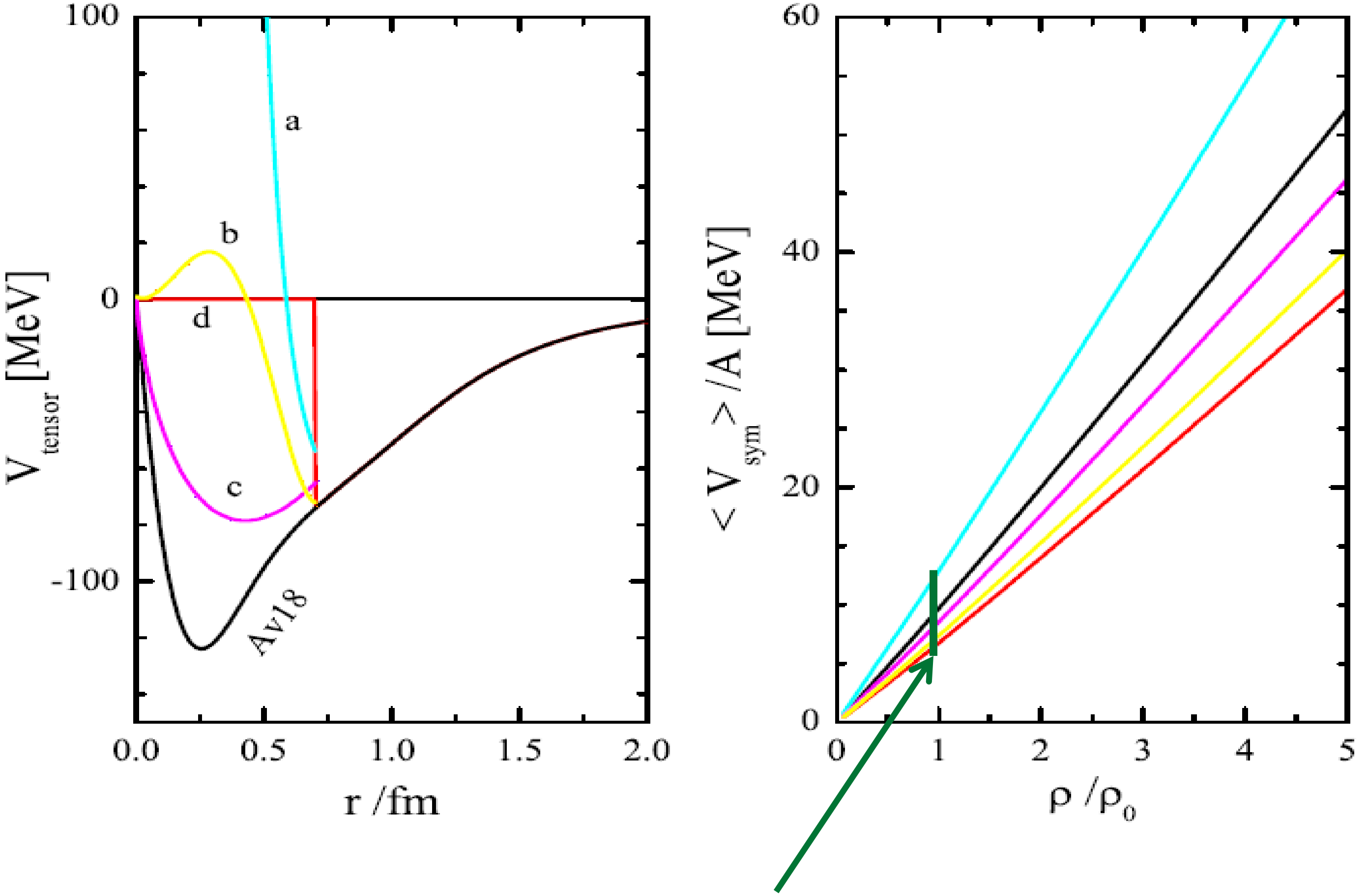

At saturation density, the 2nd order potential contribution
due to the tensor force is about 7-14 MeV, it is 9 MeV with Av18

What are the Short Range Correlations (SRC) in nuclei ?

(Modified from a slide by Eli Piasetzky)

In coordinate space:

In momentum space:

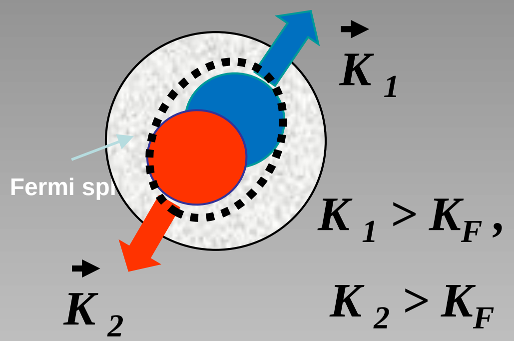

High momentum tail (HMT): (1.3 – 2.5)K_F

In isospin space:

Dominated by the isosinglet (T=0) neutron-proton pairs

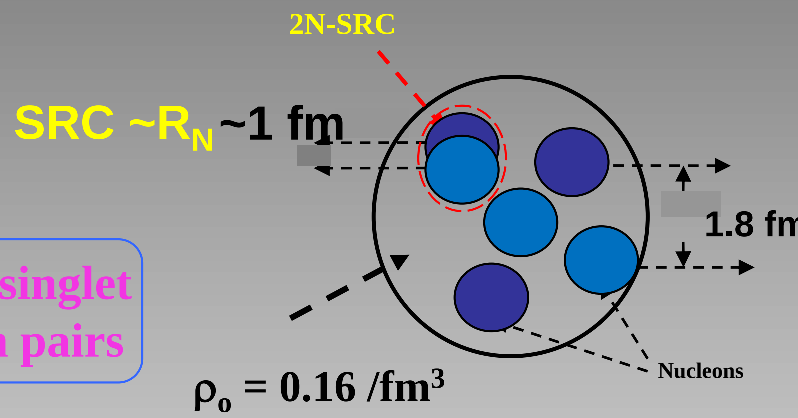

Nucleon pairs with large relative momenta and small CM momenta

Short Range Correlated pairs: temporal fluctuations of strongly interacting nucleon pairs in close proximity

Effects of the tensor force in T=0 neutron-proton interaction channel

(1) high-momentum tail (HMT) in nucleon momentum distribution

(2) isospin dependence of short-range correlation (SRC) in neutron-rich matter

H.A. Bethe
Ann. Rev. Nucl. Part. Sci., 21, 93-244 (1971)

O. Hen et al. (Jlab CLAS collaboration), Science 346, 614 (2014)

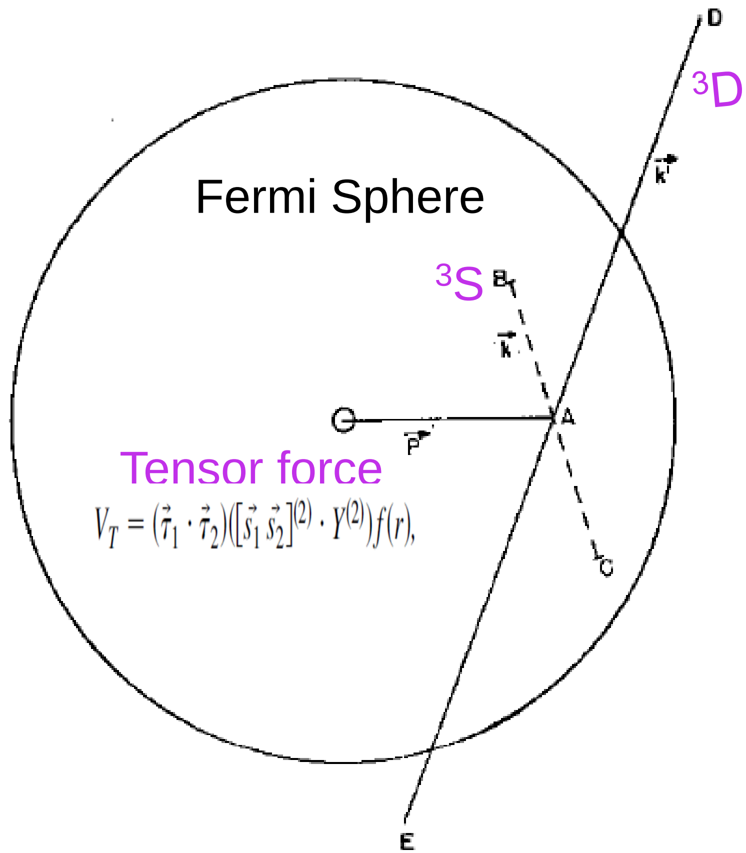

FIGURE 10. Two nucleons are initially in states B and C, having average momentum $\boldsymbol{P}$ and relative momentum $\boldsymbol{k}$. When they interact they are shifted to states D and E outside the Fermi sphere, with relative momentum $\boldsymbol{k}'$. If they are initially in a ^3S state and interact by tensor force, then they are in a $^3D_1$ state in DE.

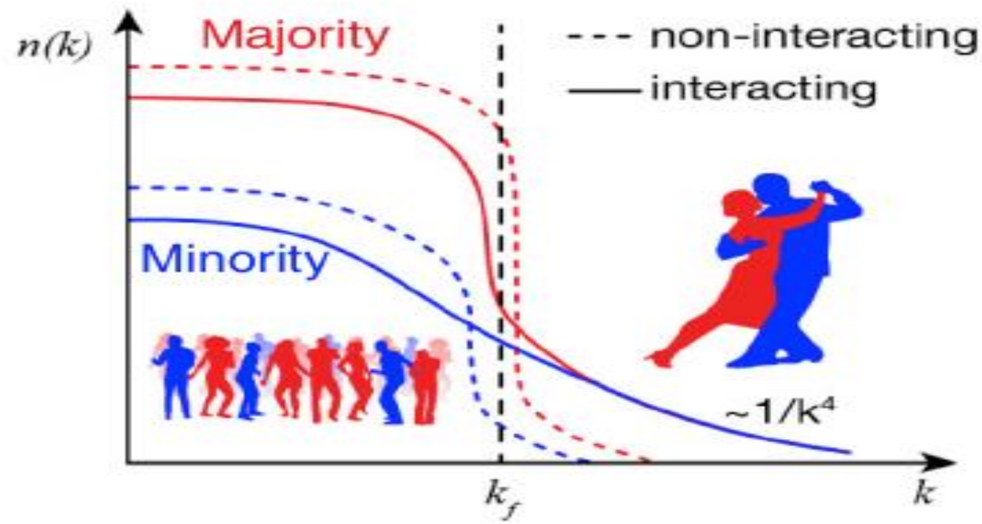

The shape, size and isospin dependence of SRC/HMT

The structure of ^{12}C in momentum space

R. B. Wiringa, R. Schiavilla, Steven C. Pieper, J. Carlson, PRC 89, 024305 (2014)

Variational Monte Carlo (VMC)

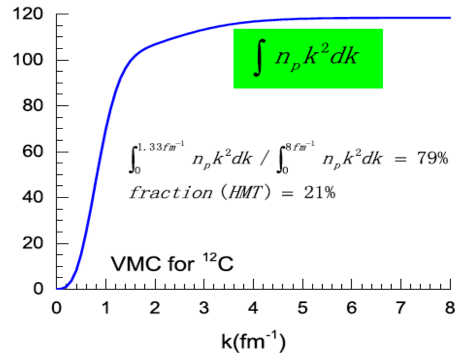

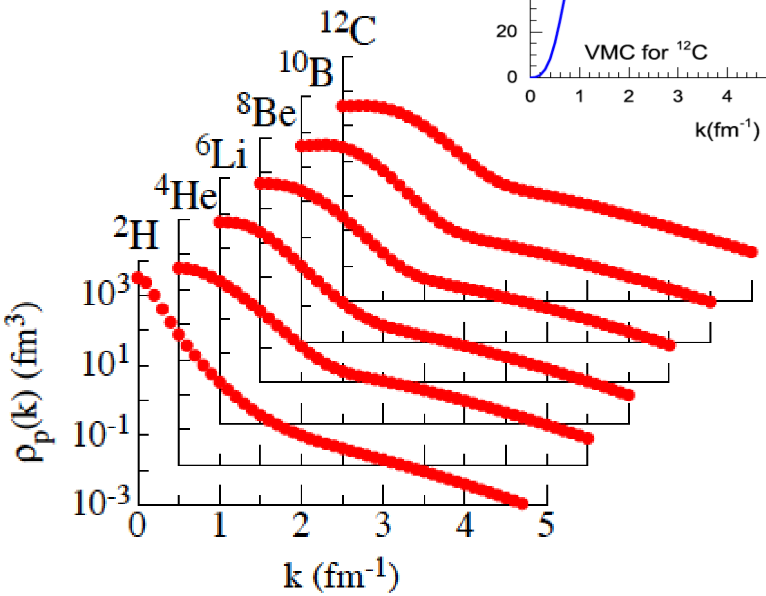

Strength and isospin dependence of SRC

R. Subedi et al. Science 320, 1475 (2008)

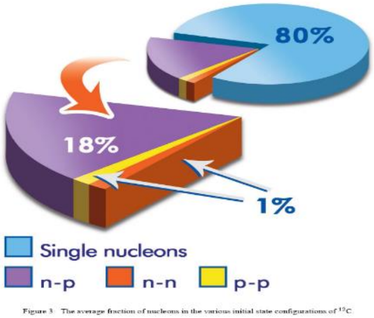

Universal high momentum tails

O. Benhar, V.R. Pandharipande, Steven C. Pieper, Rev. Modern Phys. 93 (1993) 817.

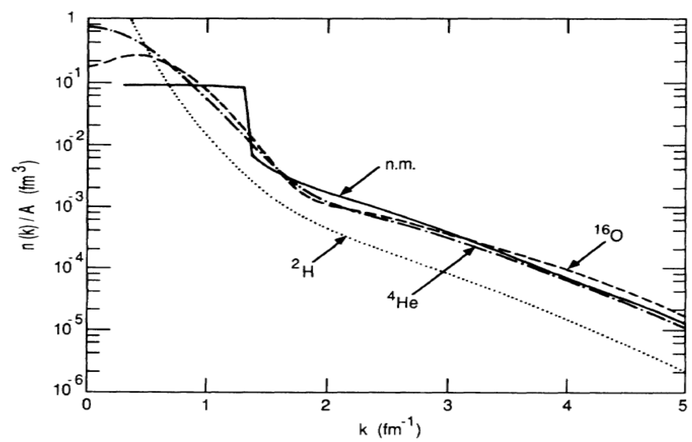

Off-shell effects in heavy particle production

Physics Letters B 367 (1996) 55–59

G.F. Bertsch [a], P. Danielewicz [b]

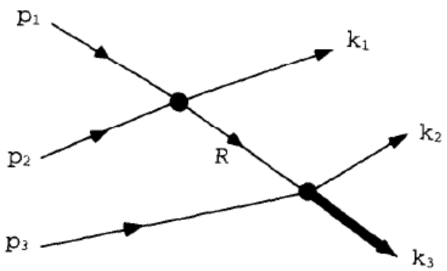

Fig. 1. The graph for heavy particle production below the two-body threshold.

$$\delta n_{\rm corr}(k) = \frac{1}{4(2\pi)^3}\int dk^0 \frac{1}{\Gamma}\frac{d^4W_{NN\to NN}}{dk^4} \approx 2\pi\sigma_{NN}\left(\frac{m^*}{m}\right)^2\frac{\rho^2}{k^4}. \qquad (9)$$

In (9) we express the NN matrix element in terms of cross section, $\sigma_{NN} = (m^2/8\pi)|M|^2$, and allow for a momentum dependence of the mean field; comparison in the figure is made for $\sigma_{NN} = 40$ mb, $m^* = m$, and $\rho = \rho_0/4$ (since we ignore the Pauli principle). The result of a complicated calculation and our expression compare favorably for $k \gg k_F$. Our result could be

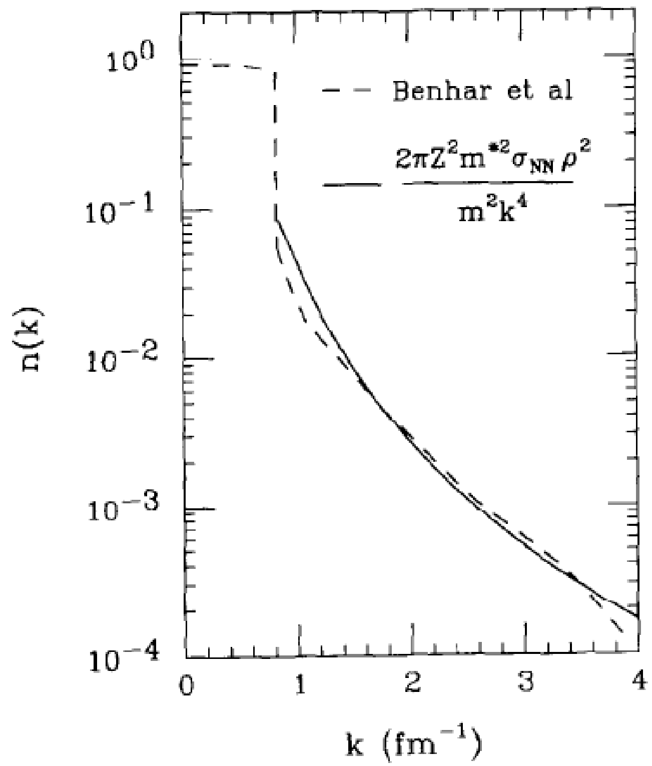

Fig. 2. Momentum occupation in nuclear matter at $\rho = \rho_0/4$. The solid line is our result, Eq. (9), applicable for $k > k_F$. The dashed line is the result of Ref. [9], including the region for $k < k_F$ as well as correlation contribution for $k > k_F$.

The high momentum tail in dilute Fermi gas at zero temperature due to the repulsive core

A.B. Migdal, *The momentum distribution of interacting Fermi particles*, Sov. Phys. JETP, 333 (1957)

Universal for all 2-component fermion systems

(1)From 2nd-order perturbation theory with a repulsive interaction

(2)The shape of HMT is universal-→ $(K_F/k)^4$

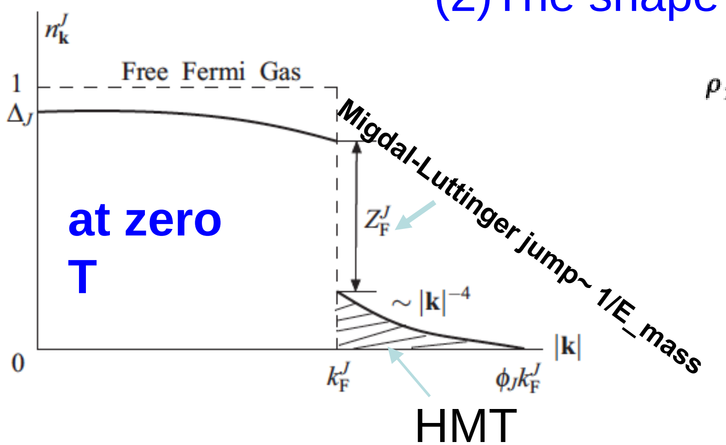

$x = k/k_F$

$$\rho_>(k) = \frac{\nu-1}{6\pi^2 x}(k_F c)^2 \Big\{ (7x^3-3x-6)\ln\frac{x-1}{x+1} + (7x^3-3x+2)\ln 2 - 8x^3+22x^2+6x-24-4(x^2-2)^{3/2} \times \left[\tan^{-1}\frac{x+2}{(x^2-2)^{1/2}} + \tan^{-1}(x^2-2)^{-1/2} - 2\tan^{-1}x(x^2-2)^{-1/2} \right] \Big\} .$$

(3) The fraction of HMT $N_>/N = \frac{8}{5}\frac{\nu-1}{\pi^2}(k_F c)^2$

All HMT nucleons are on shell $\epsilon(k) = k^2/2m + V(k;\epsilon(k))$

V. A. Belyakov, Sov. Phys. JETP 13, 850 (1961).

R. Sartor and C. Mahaux, Phys. Rev. C 21, 1546 (1981)

R. Amado, Phys. Rev. C 14, 1264 (1976).

S.N. Tan, Ann. Phys. 323, 2952 (2008); 323, 2971 (2008); 323, 2987 (2008).

S. K. Bogner and D. Roscher, Phys. Rev. C 86, 064304 (2012)

A. Rios, A. Polls, and W.H. Dickhoff, Phys. Rev. C 89, 044303 (2014).

Experimental evidence of isospin-dependent nucleon momentum distribution:
Deformed-Fermi distributions in neutron-rich matter

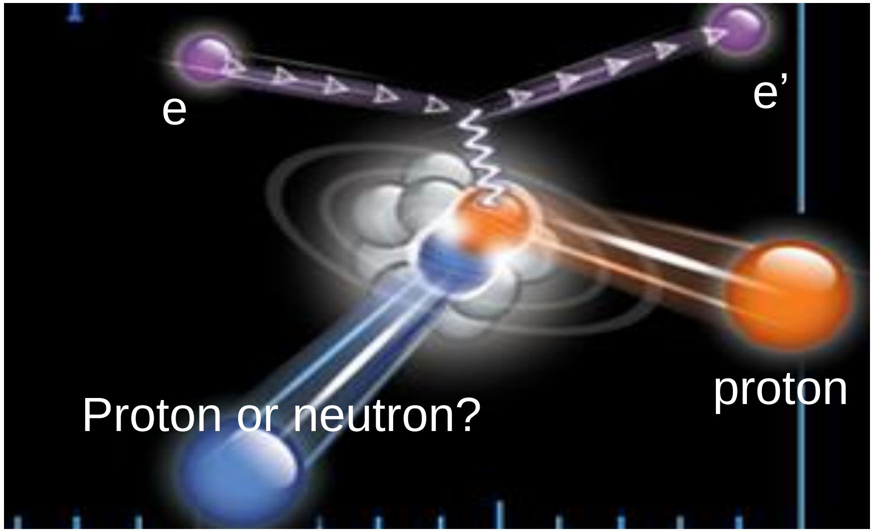

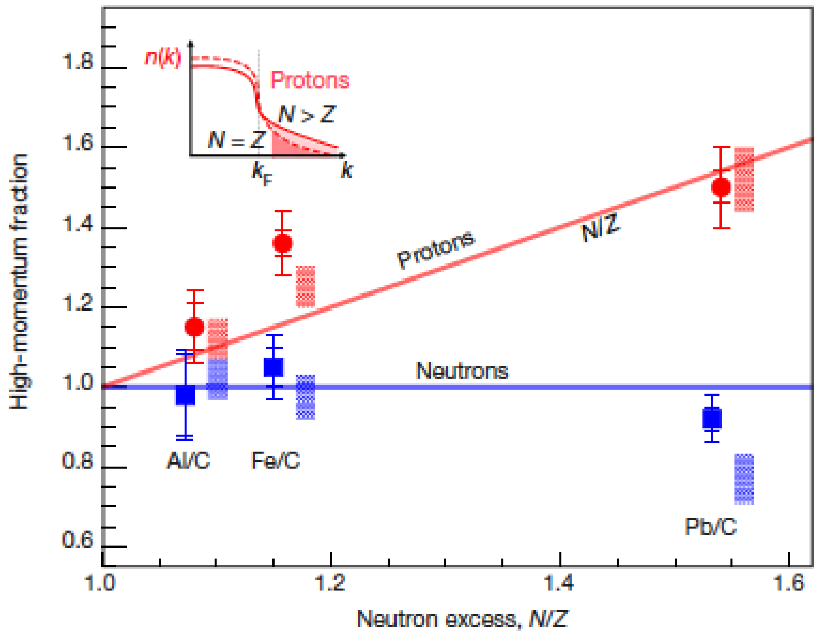

M. Duer et al., Nature 560, 617 (2018).

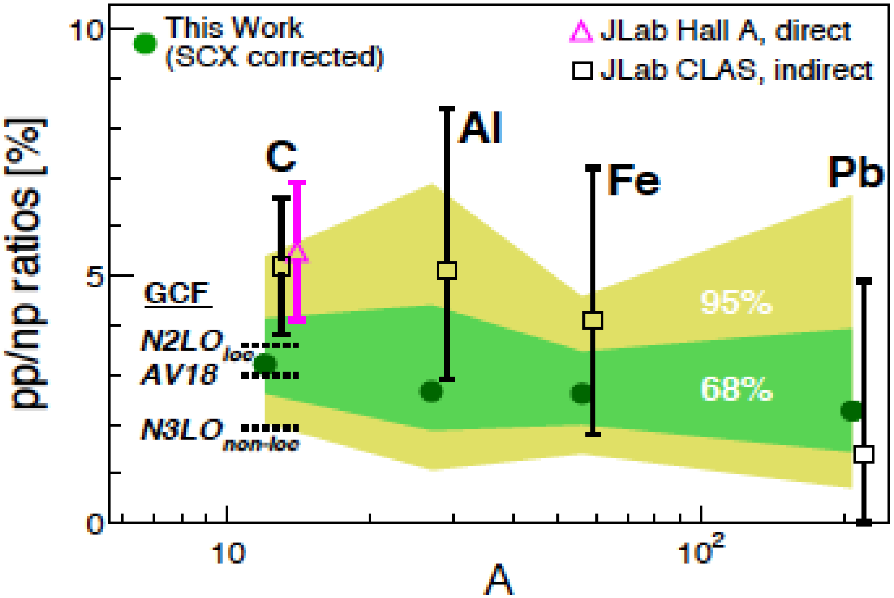

M. Duer et al., PRL 122, 172502 (2019).

Effects of isospin-dependent SRC on the kinetic symmetry energy of quasi-nucleons

Chang Xu, Ang Li and Bao-An Li,
JPCS 420, 012190 (2013).

$$E_{kin} = \alpha \int_0^{\infty} \frac{\hbar^2 k^2}{2m} n(k) k^2 dk,$$

Free-Fermi Gas (FFG):
kinetic E_{sym}=12.3 MeV at ρ_0

$$E_{sym}^{kin} = E_{PNM}^{kin} - E_{SNM}^{kin} < 0$$

if more than 15% nucleons are in the high-momentum tail of SNM due to the tensor force for n-p T=0 channel, the kinetic symmetry energy becomes negative

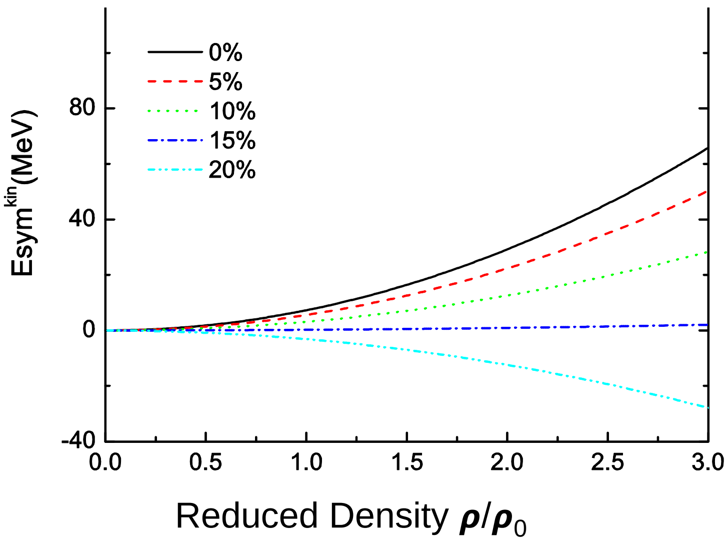

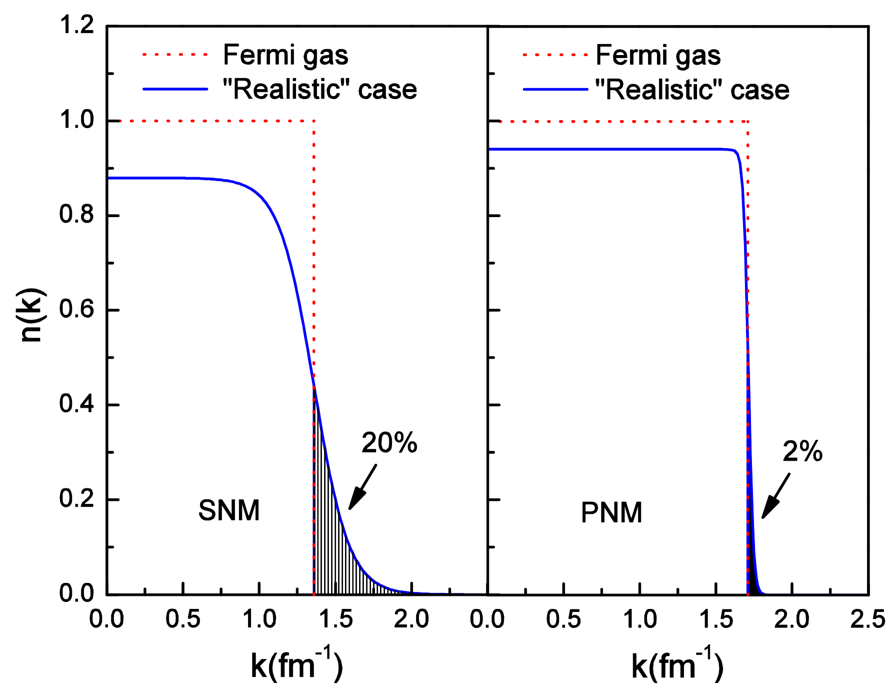

Confirmation by Microscopic Many-Body Theories

1. Isaac Vidana, Artur Polls, Constanca Providencia
PRC84, 062801(R) (2011)

Brueckner--Hartree--Fock approach using the Argonne V18 potential
plus the Urbana IX three-body force

2. Arianna Carbone, Artur Polls, Arnau Rios, EPL 97, 22001 (2012)
A. Carbone, A. Polls, C. Providência, A. Rios, I. Vidaña, EPJA 50, 13 (2014)
Self-Consistent Green's Function Approach with Argonne Av18, CDBonn, Nij1, N3LO interactions

3. Alessandro Lovato, Omar Benhar et al.,
extracted from results already published in
Phys. Rev. C83:054003,2011
Using Argonne V'_6 interaction
Fermi-Hyper-Netted-Chain (FHNC)
Single Operator Chains (SOC)

4. A. Rios, A. Polls, W. H. Dickhoff
PRC 89, 044303 (2014).
Ladder Self-Consistent Green Function

Brueckner--Hartree—Fock prediction

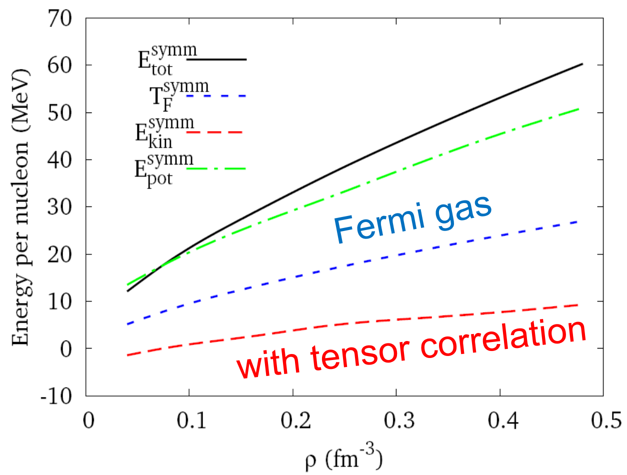

They all included the tensor force and
many-body correlations using different techniques

Self-Consistent Green's Function Approach (A. Rios et al.)

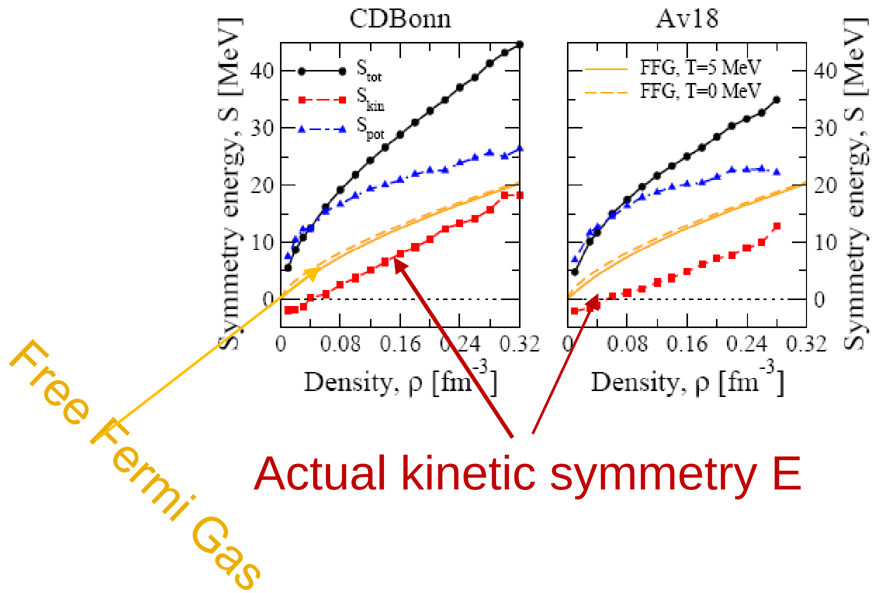

	$S_{\rm tot}$ [MeV]	$S_{\rm kin}$ [MeV]	$S_{\rm pot}$ [MeV]	L [MeV]
Av18	25.1	4.9	20.2	37.7
Nij1	27.4	4.6	22.8	48.5
CDBonn	28.8	7.9	20.9	52.6
N3LO	29.7	7.2	22.4	55.2

Brueckner–Hartree–Fock approach (I. Vidana et al.

Using the Hellmann–Feynman theorem

V18 potential plus the Urbana IX three-body force.

At saturation density,
the Free Fermi Gas (FFG) model
prediction is about 12.5 MeV

	E_{NM}	E_{SM}	E_{sym}	L
$\langle T \rangle$	53.321	54.294	−0.973	14.896
$\langle V \rangle$	−34.251	−69.524	35.273	51.604
Total	19.070	−15.230	34.300	66.500

Reduced Kinetic symmetry energy of quasi-nucleons due to the isospin dependence of SRC

Free-Fermi Gas (FFG): $E_{sym}^{kin}(r) = \frac{1}{3} E_F(r_0)(r / r_0)^{2/3} \approx 12.5\,\text{MeV at } r_0$

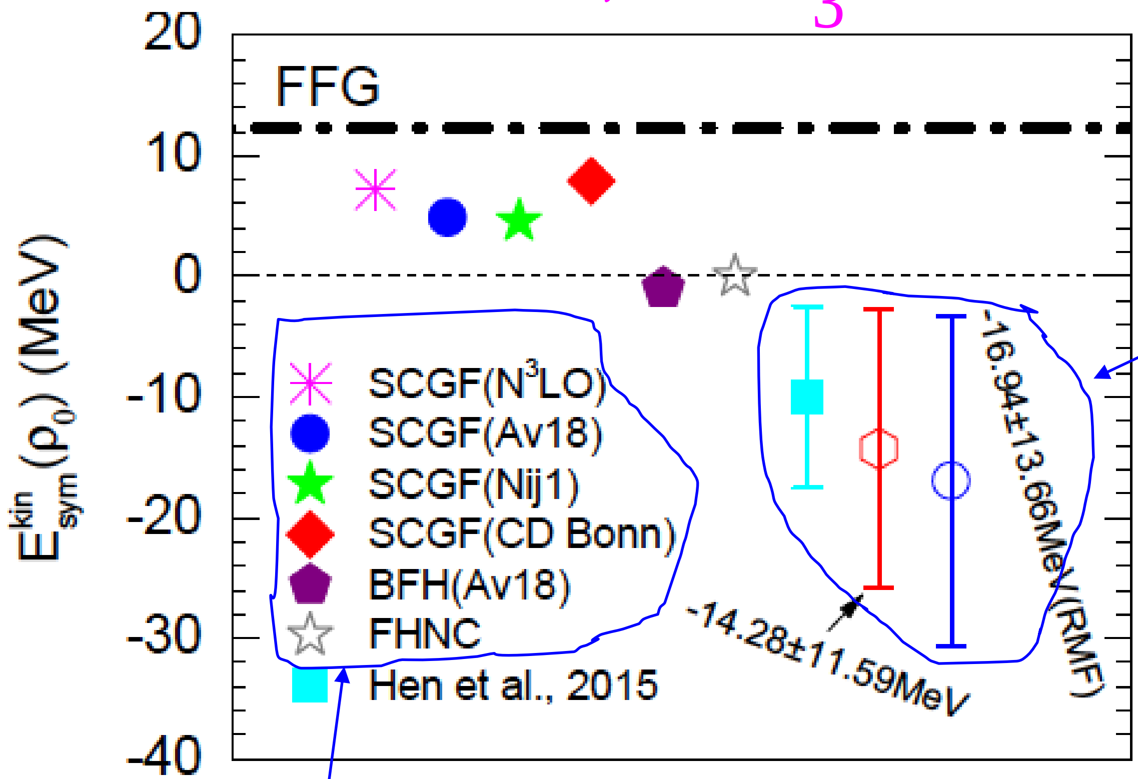

Extracted from SRC data using the n-p dominance model

Microscopic Many-Body Theories with SRC

O. Hen, B.A. Li, W.J. Guo, L.B. Weinstein, E. Piasetzky, Phys. Rev. C 91 (2015) 025803.

B.A. Li, W.J. Guo, Z.Z. Shi, Phys. Rev. C 91 (2015) 044601.

B.J. Cai, B.A. Li, Phys. Rev. C 92 (2015) 011601(R).

Modified Gogny Hartree-Fock energy density functional incorporating SRC-induced high momentum tail in the single nucleon momentum distribution

Kinetic **Zero-range Two-body force** **Three-body force**

$$E(\rho,\delta) = E^{\mathrm{kin}}(\rho,\delta) + \frac{A_\ell(\rho_{\mathrm{p}}^2+\rho_{\mathrm{n}}^2)}{2\rho\rho_0} + + \frac{A_{\mathrm{u}}\rho_{\mathrm{p}}\rho_{\mathrm{n}}}{\rho\rho_0} + \frac{B}{\sigma+1}\left(\frac{\rho}{\rho_0}\right)^\sigma(1-x\delta^2)$$
$$+ \sum_{J,J'}\frac{C_{J,J'}}{\rho\rho_0}\int \mathrm{d}\mathbf{k}\mathrm{d}\mathbf{k}' f_J(\mathbf{r},\mathbf{k}) f_{J'}(\mathbf{r},\mathbf{k}')\Omega(\mathbf{k},\mathbf{k}'),$$

$$\Omega(\mathbf{k},\mathbf{k}') = \left[1+\frac{(\mathbf{k}-\mathbf{k}')^2}{\Lambda^2}\right]^{-1}$$

Momentum-dependent potential energy due to finite-range 2-body interaction

C. B. Das, S. Das Gupta, C. Gale, Bao-An Li Phys.Rev.C67:034611,2003

$$\int_0^{k_{\mathrm{F}}^J}(\text{FFG step function})\, f\, d\mathbf{k} \longrightarrow \int_0^{\phi_J k_{\mathrm{F}}^J} n_{\mathbf{k}}^J\,(\text{HMT})\, f\, d\mathbf{k}.$$

$$E^{\mathrm{kin}}(\rho,\delta) = \sum_{J=\mathrm{n,p}}\frac{1}{\rho_J}\int_0^\infty \frac{\mathbf{k}^2}{2M} n_{\mathbf{k}}^J(\rho,\delta)\mathrm{d}\mathbf{k}$$

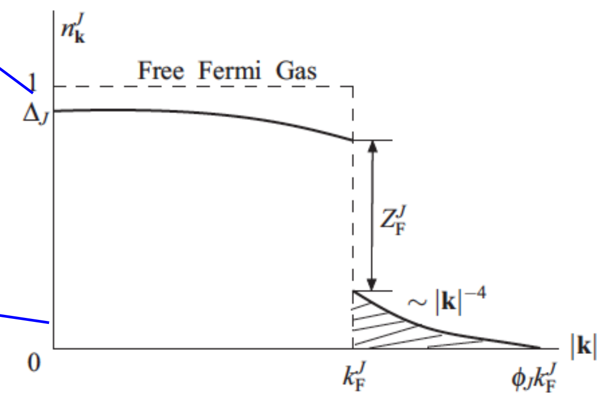

SRC-induced HMT in the single-nucleon momentum distribution affects both the kinetic energy and the momentum-dependent part of the potential energy

Readjusting model parameters to reproduce the same saturation properties of nuclear matter as well as $E_{sym}(\rho_0)$=31.6 MeV and $L(\rho_0)$=58.9 MeV

Consequence: Symmetry energy gets softened at both low and high densities

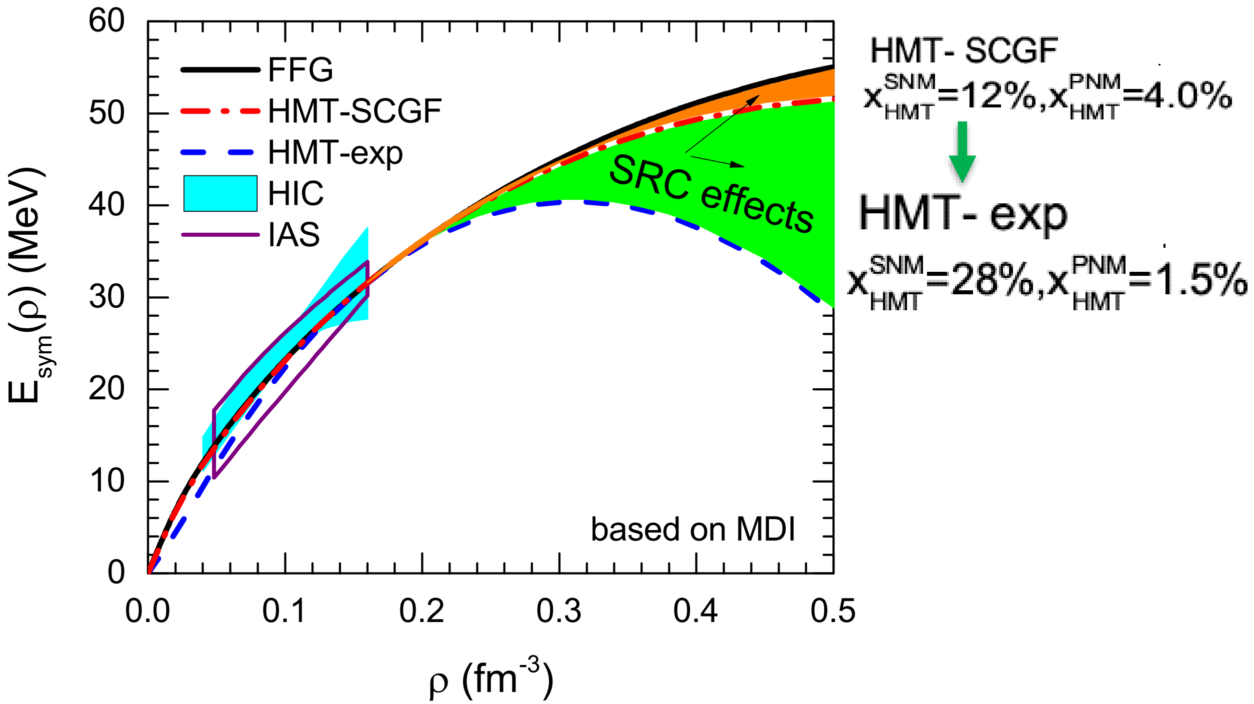

Bao-Jun Cai, Bao-An Li and Lie-Wen Chen,

AIP Conference Proceedings 2038, 020041 (2018)

Neutron-skin in ^{208}Pb and $dE_{sym}/d\rho$

Earlier work: B.A. Brown, S. Typel, C. Horowitz, J. Piekarewicz, R.J. Furnstahl, J.R. Stone, A. Dieperink et al.

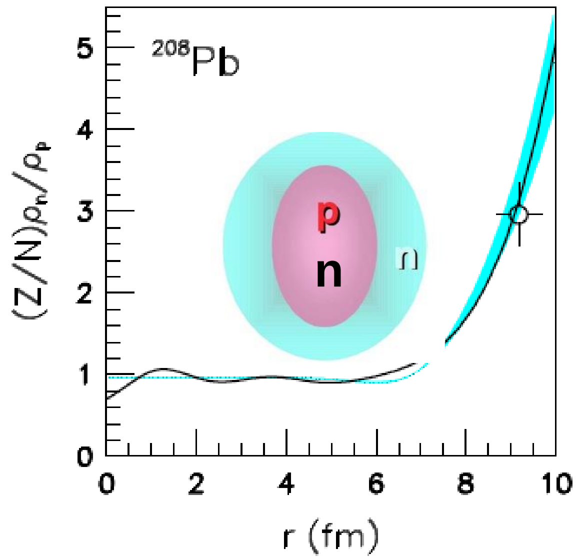

P.Pawłowski and A. Szczurek, PRC 70, 044908 (2004)

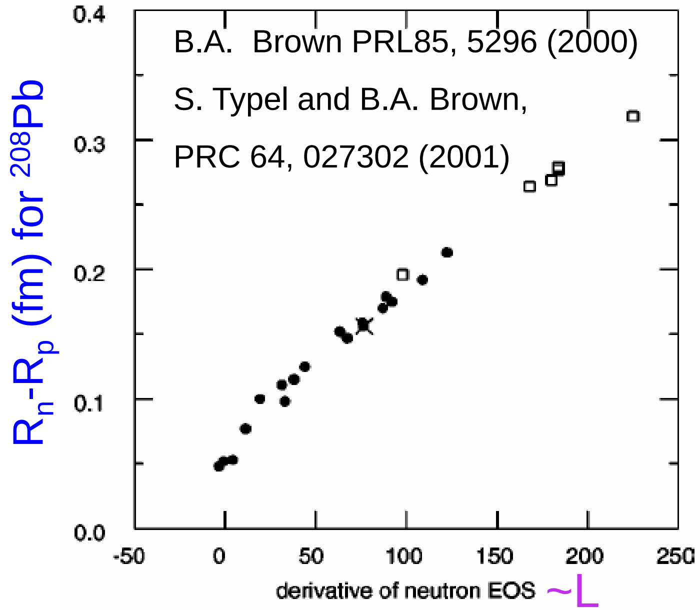

$$E_{neutron} = E_{nuclear} + E_{sym},$$

$$R_n - R_p \propto \Delta p_{np} = dE_{nuclear}/d\rho|_{\rho_0} + dE_{sym}/d\rho|_{\rho_0} = 0 + dE_{sym}/d\rho|_{\rho_0}$$

Pressure forces neutrons out against the surface tension from the symmetric core near ρ_0

$$P = \rho^2 \frac{d}{d\rho}\frac{E}{A} \simeq \frac{L}{3\rho_0}\rho^2 \quad \rightarrow \text{n-skin} \sim L$$

Neutron-skin is actually determined by $L(\sim 2\rho_0/3)$ NOT $L(\rho_0)$

Z. Zhang and L. W. Chen, Phys. Lett. B 726, 234 (2013)

- **Extrapolation from $L(2\rho_0/3)$ to $L(\rho_0)$ is very model dependent**
- **The correlation between n-skin of heavy nuclei and the radius of neutron stars is also VERY model dependent**

Why there are neutron skins in heavy nuclei

To minimize the total energy

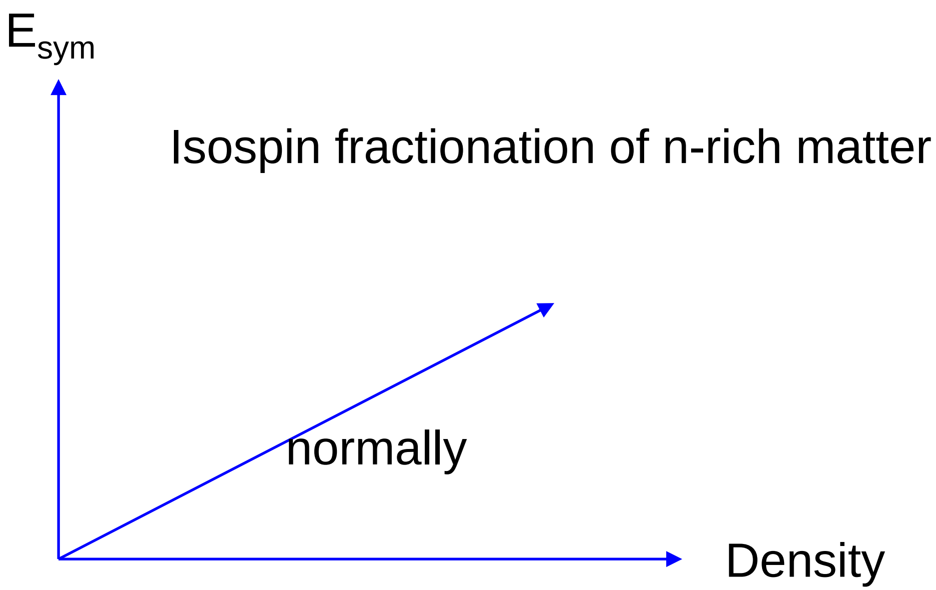

Big, small at high densities

$$E(\rho,\delta) = E(\rho,0) + E_{sym}(\rho)\delta^2$$

Small, big at low densities

Transport model simulation of neutron-rich matter in a box

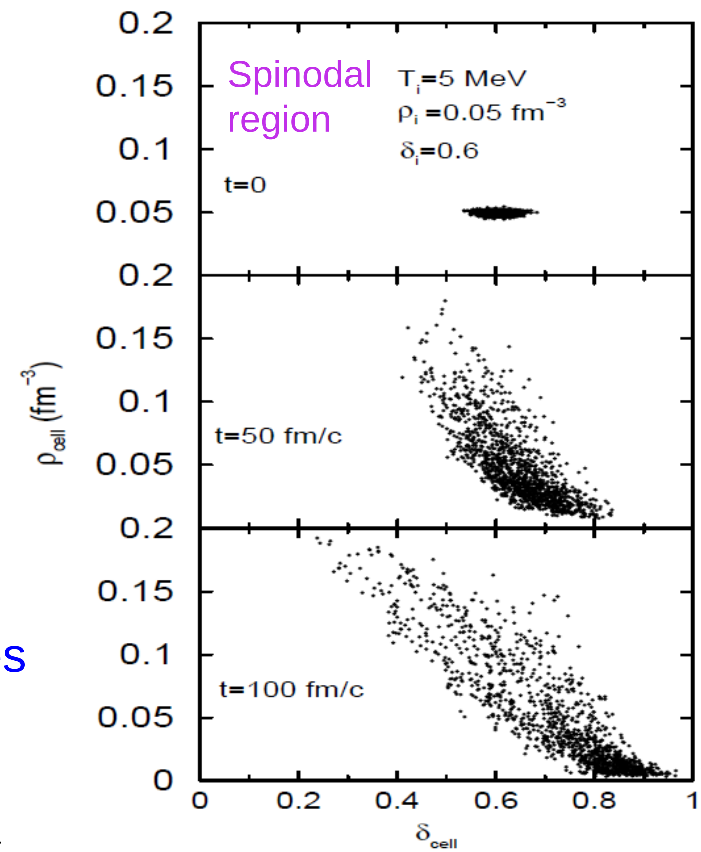

BA Li, AT Sustich, M Tilley, B Zhang
PRC 64, 051303 (2001)

Isospin fraction during heavy-ion reactions

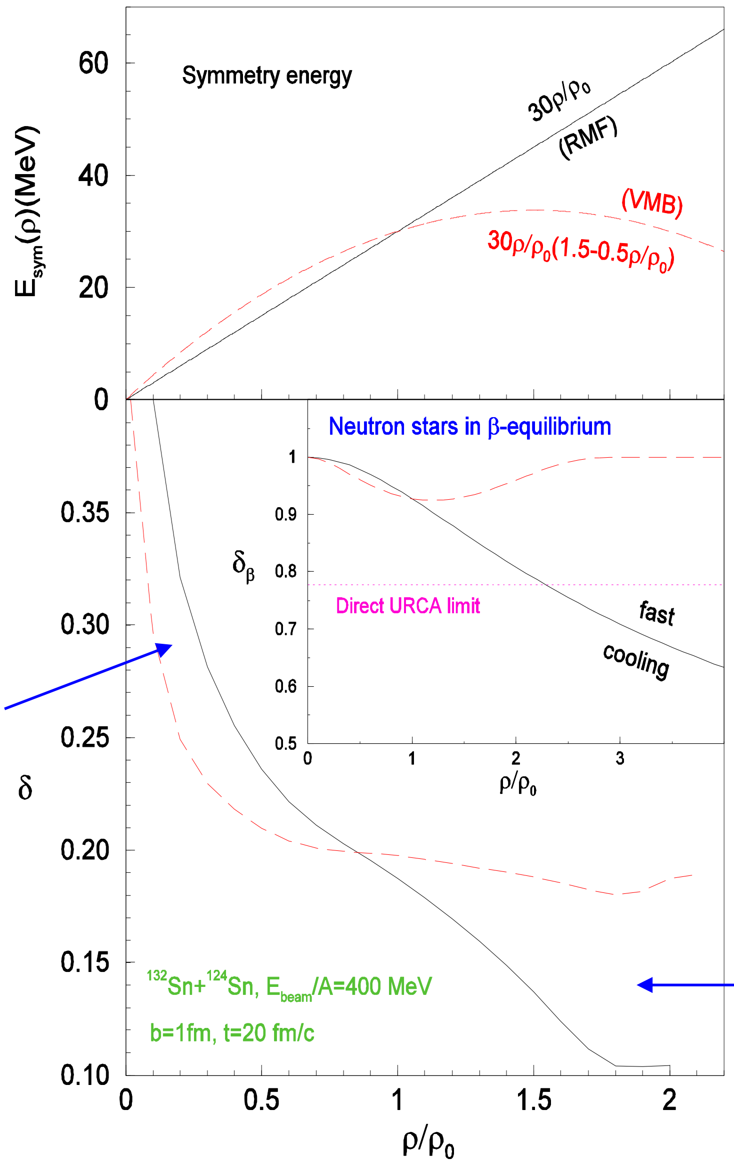

$$E(\rho,\delta) = E(\rho,0) + E_{sym}(\rho)\delta^2$$

high density region is more neutron-rich with soft symmetry energy

n/p spectrum ratio of pre-equilibrium emission probing neutron-proton effective mass splitting

The density dependence of isospin asymmetry in neutron stars and heavy-ion reactions are similar

π^-/π^+ ratio at freeze-out and neutron-proton differential flow probing high-density E_{sym}

Bao-An Li, Phys. Rev. Lett. 88 (2002) 192701

Microscopic diagnosis of n-skins in two Skyrme-Hartree-Fock models with similar EOSs for SNM and E_{sym} as the APR up to $1.5\rho_0$

$$S_1(\rho) = \frac{\hbar^2 k_F^2}{6m_0^*(\rho, k_F)}$$
$$S_2(\rho) = \frac{1}{2}U_{sym,1}(\rho, k_F) \ ,$$
$$L_1(\rho) = \frac{2\hbar^2 k_F^2}{6m_0^*(\rho, k_F)} \equiv 2S_1(\rho)$$
$$L_2(\rho) = -\frac{\hbar^2 k_F^3}{6m_0^{*2}(\rho, k_F)} \frac{\partial m_0^*(\rho, k)}{\partial k}\bigg|_{k=k_F}$$
$$L_3(\rho) = \frac{3}{2}U_{sym,1}(\rho, k_F) \equiv 3S_2(\rho)$$
$$L_4(\rho) = \frac{\partial U_{sym,1}(\rho, k)}{\partial k}\bigg|_{k=k_F} \cdot k_F$$
$$L_5(\rho) = 3U_{sym,2}(\rho, k_F) \ .$$

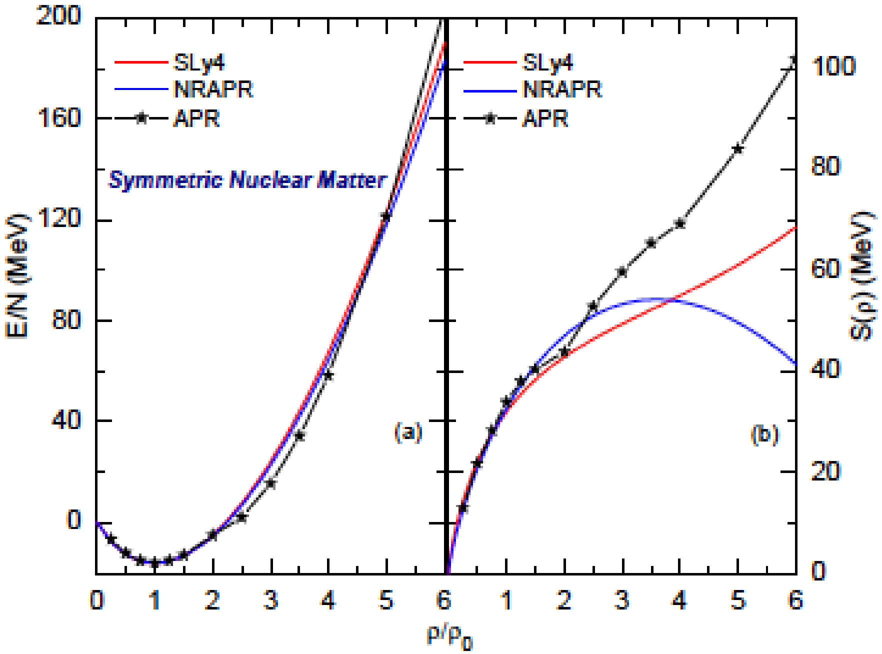

L_Sly4 = 45.9 MeV
L_NRAPR = 59.6 MeV

For ^{208}Pb
Rskin_Sly4 = 0.157 fm
Rskin_NRAPR = 0.184 fm

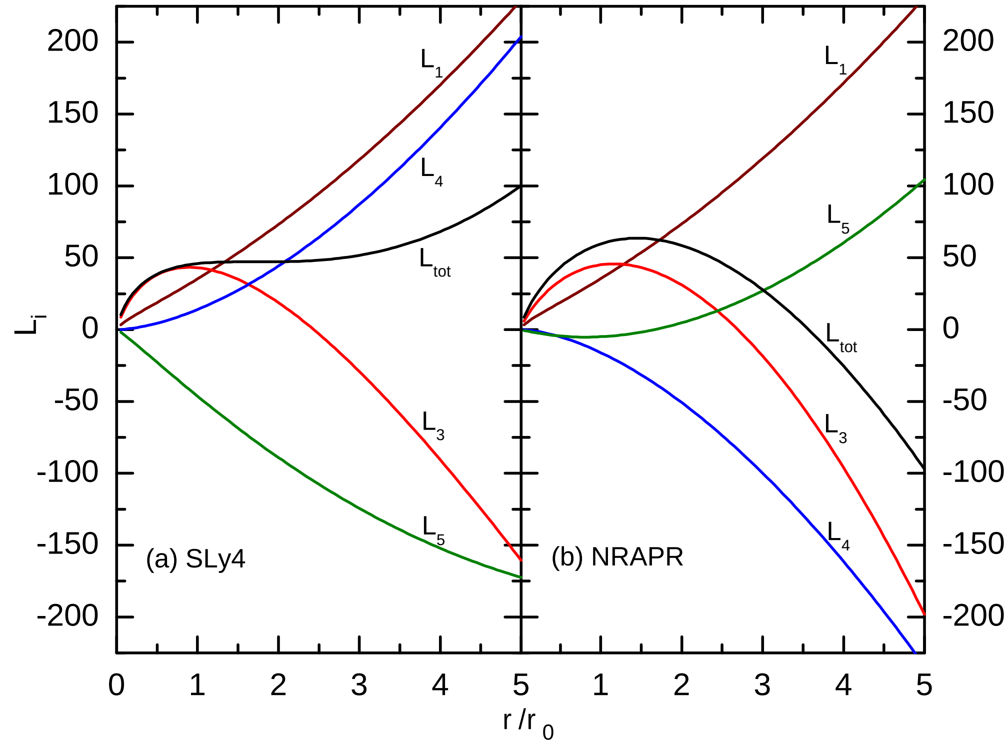

F. Fattoyev, W.G. Newton and Bao-An Li
PRC 90, 022801(R) (2014)

$$E_{sym}(\rho) = \frac{1}{3}\frac{\hbar^2 k^2}{2m_0^*}|_{k_F} + \frac{1}{2}U_{sym,1}(\rho,k_F),$$

$$L(\rho) = \frac{2}{3}\frac{\hbar^2 k^2}{2m_0^*}|_{k_F} - \frac{1}{6}\left(\frac{\hbar^2 k^3}{m_0^{*2}}\frac{\partial m_0^*}{\partial k}\right)|_{k_F} + \boxed{\frac{3}{2}U_{sym,1}(\rho,k_F)} + \frac{\partial U_{sym,1}}{\partial k}|_{k_F}\cdot k_F + 3U_{sym,2}(\rho,k_F),$$

L_1 L_2 L_3 L_4 L_5

Covariance analysis of the correlation between n-skin and $L_i(\rho)$

$$C(X,Y) = \frac{\langle (X-\langle X\rangle)(Y-\langle Y\rangle)\rangle}{\sqrt{\langle (X-\langle X\rangle)^2\rangle\langle (Y-\langle Y\rangle)^2\rangle}}$$

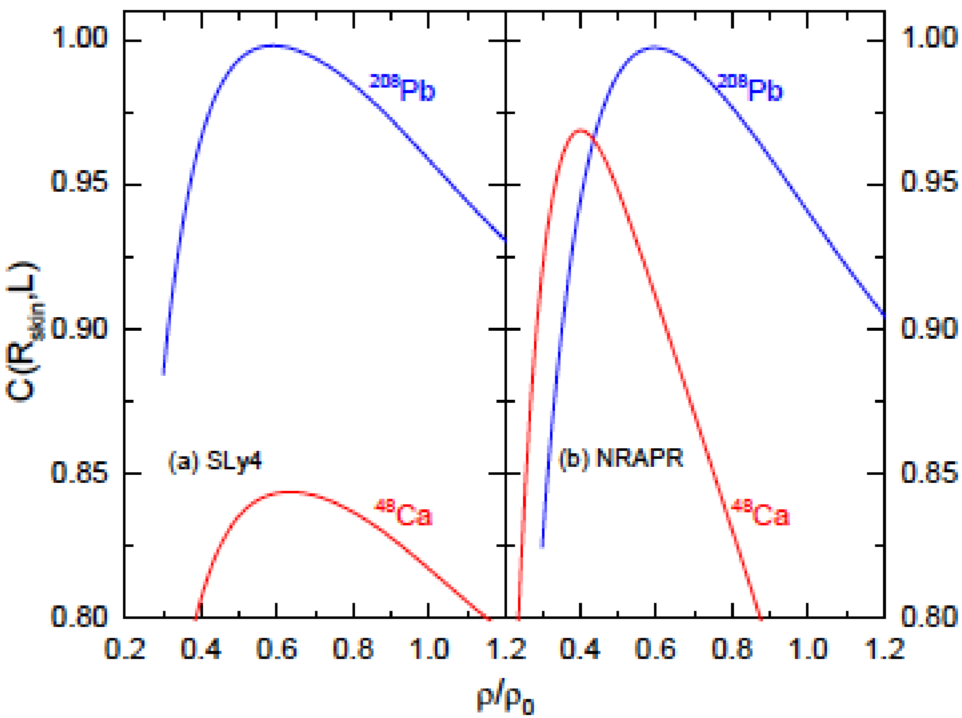

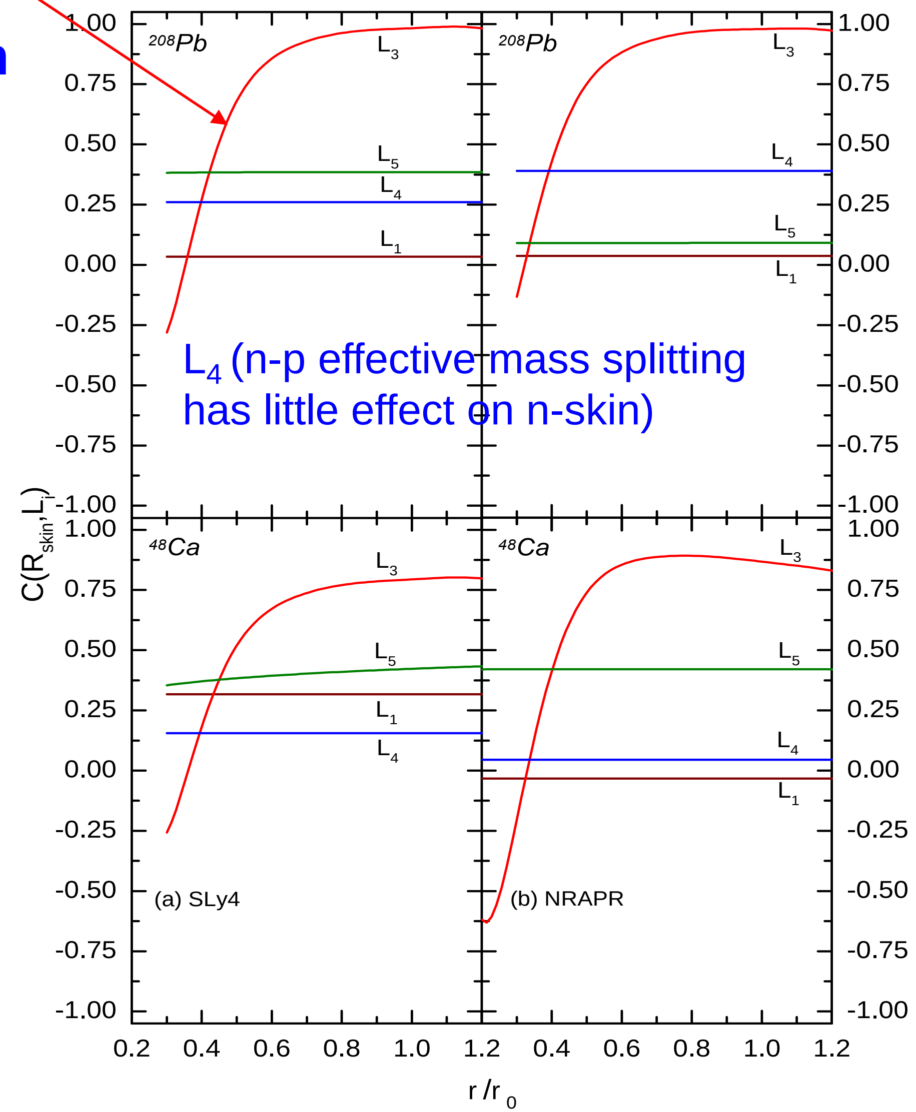

Symmetry energy and single nucleon potential MDI used in the IBUU04 transport model

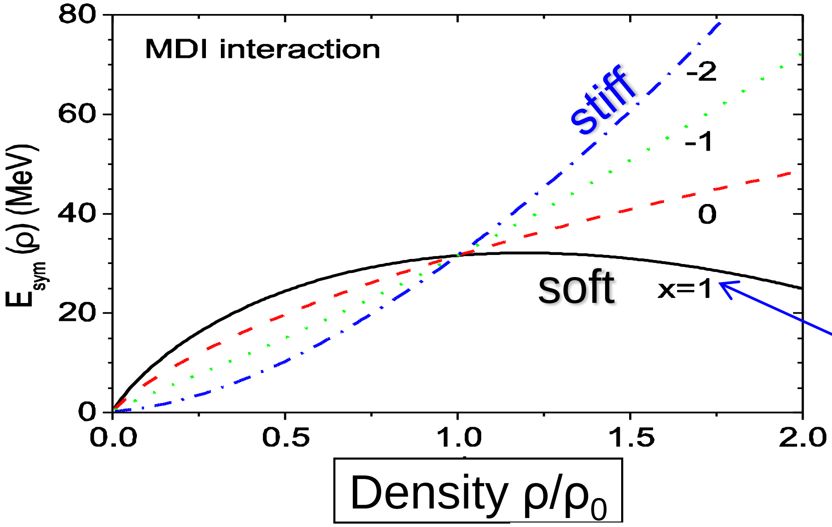

The x parameter is introduced to mimic various predictions on the symmetry energy by different microscopic nuclear many-body theories using different effective interactions.

It is the coefficient of the 3-body force term

Default: Gogny force

Potential energy density

$$V(\rho,\delta) = \frac{A_1}{2\rho_0}\rho^2 + \frac{A_2}{2\rho_0}\rho^2\delta^2 + \frac{B}{\sigma+1}\frac{\rho^{\sigma+1}}{\rho_0^\sigma}(1 - x\delta^2) + \frac{1}{\rho_0}\sum_{\tau,\tau'} C_{\tau,\tau'}\int\int d^3p\, d^3p' \frac{f_\tau(\vec{r},\vec{p}) f_{\tau'}(\vec{r},\vec{p}')}{1+(\vec{p}-\vec{p}')^2/\Lambda^2}$$

Single nucleon potential within the HF approach using a modified Gogny force:

$$U(\rho,\delta,\vec{p},\tau,x) = A_u(x)\frac{\rho_{\tau'}}{\rho_0} + A_l(x)\frac{\rho_\tau}{\rho_0} + B\left(\frac{\rho}{\rho_0}\right)^\sigma(1 - x\delta^2) - 8\tau x\frac{B}{\sigma+1}\frac{\rho^{\sigma-1}}{\rho_0^\sigma}\delta\rho_{\tau'}$$
$$+ \frac{2C_{\tau,\tau}}{\rho_0}\int d^3p' \frac{f_\tau(\vec{r},\vec{p}')}{1+(\vec{p}-\vec{p}')^2/\Lambda^2} + \frac{2C_{\tau,\tau'}}{\rho_0}\int d^3p' \frac{f_{\tau'}(\vec{r},\vec{p}')}{1+(\vec{p}-\vec{p}')^2/\Lambda^2}$$

$$\tau,\tau' = \pm\frac{1}{2},\quad A_l(x) = -121 + \frac{2Bx}{\sigma+1},\quad A_u(x) = -96 - \frac{2Bx}{\sigma+1},\quad K_0 = 211\,MeV$$

C.B. Das, S. Das Gupta, C. Gale and B.A. Li, PRC 67, 034611 (2003).

B.A. Li, C.B. Das, S. Das Gupta and C. Gale, PRC **69**, 034614; NPA **735**, 563 (2004).

Probing the symmetry energy at supra-saturation densities

$$E(\rho,\delta) = E(\rho,0) + E_{sym}(\rho)\delta^2$$

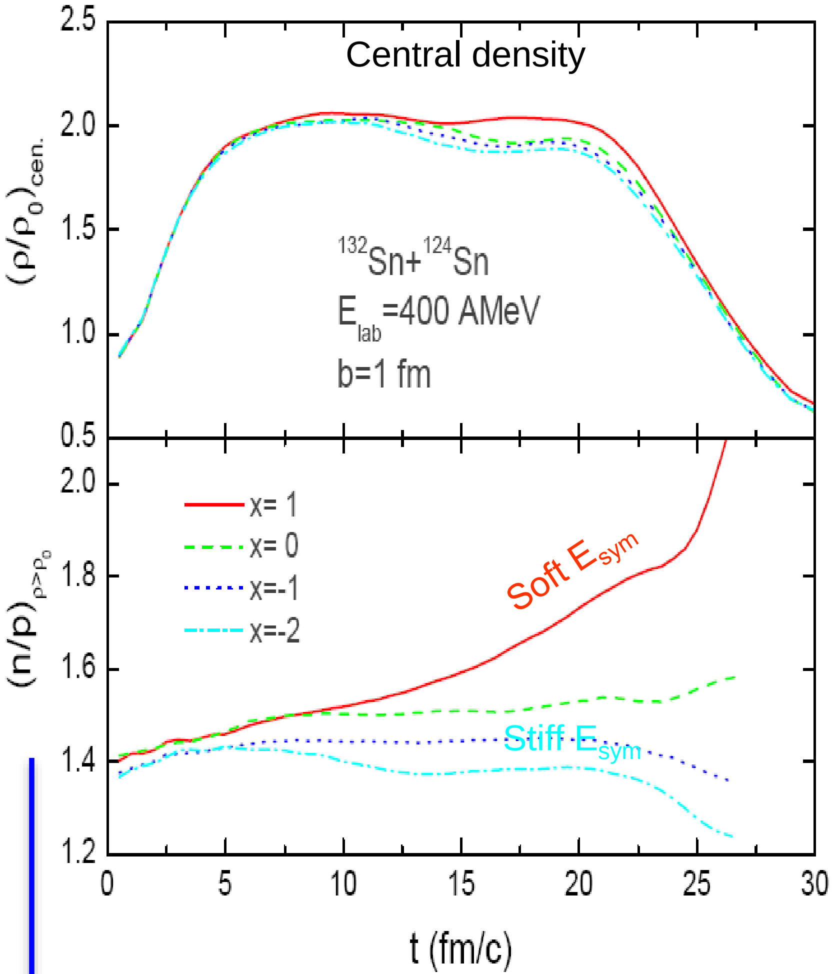

Symmetry energy

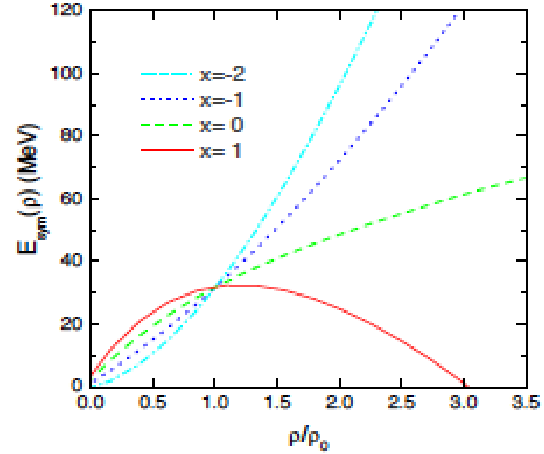

π⁻/ π⁺ probe of dense matter

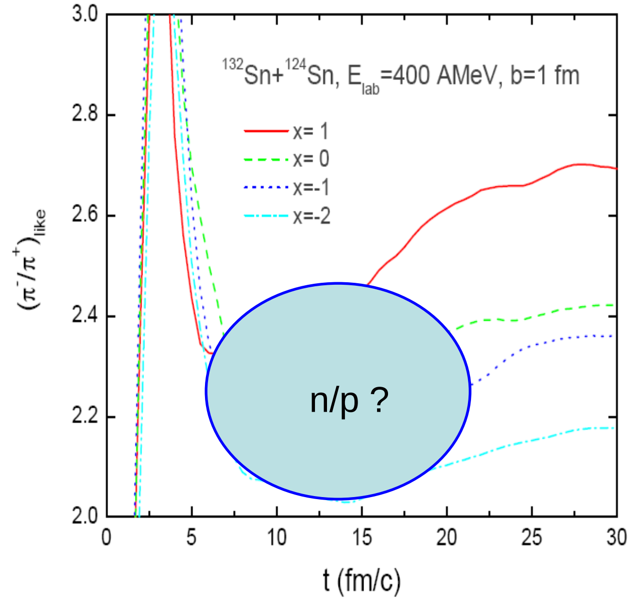

n/p ratio at supra-saturation densities

Influence of neutron-skin thickness on π^-/π^+ ratio in Pb+Pb collisions

Gao-Feng Wei,[1,2,*] Bao-An Li,[1,3,†] Jun Xu,[4,‡] and Lie-Wen Chen[5,6,§]

PRC 90 (2014), 014610

n-skin from SHF for the initial state

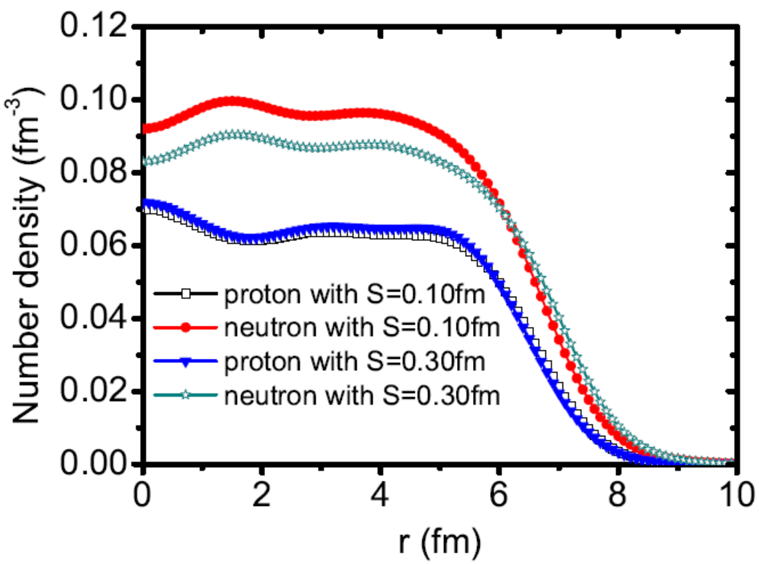

n-sin of target/proj.–like nuclei during HIC

two surfaces
are 3 fm apart
at t=0

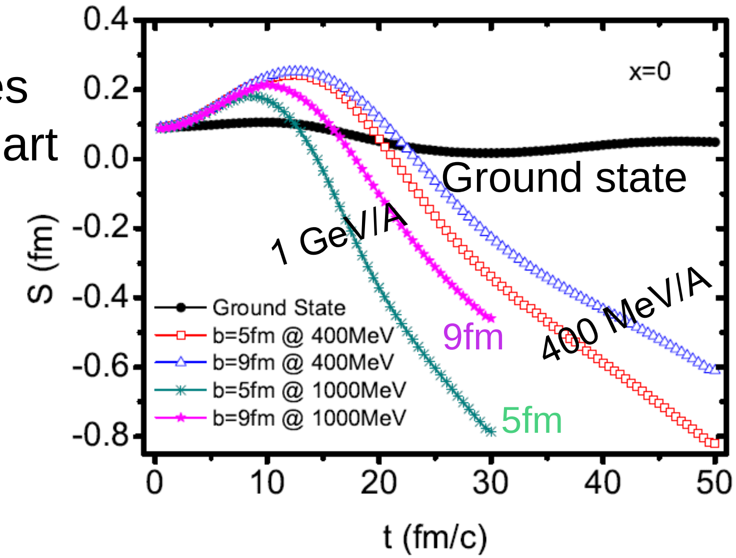

Negative pions are produced earlier
from the overlapping neutron skins

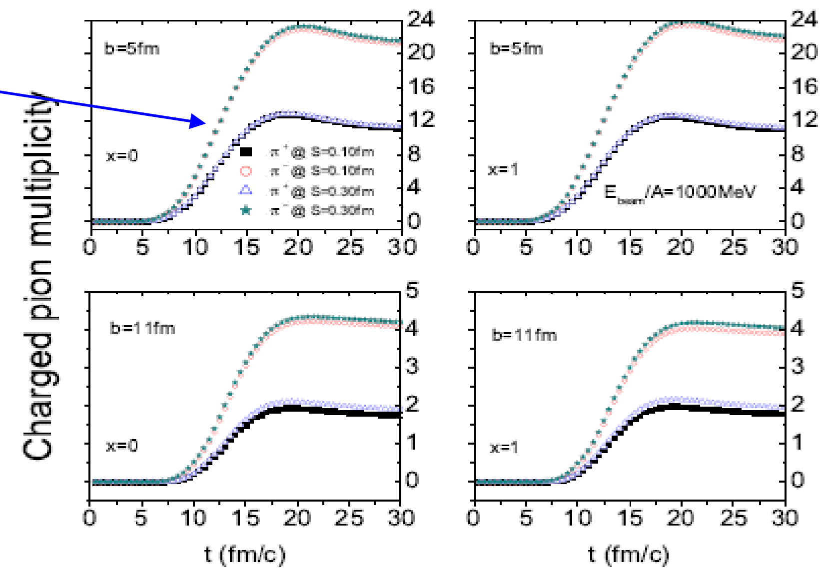

x-parameter: controls the spin-isospin dependence of 3-body force in Gogny-HF EDF

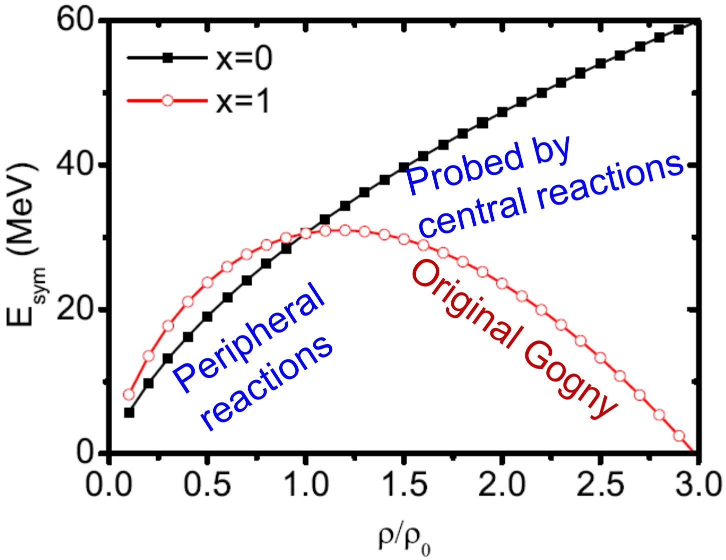

Single-particle potential

$$
\begin{aligned}
U(\rho,\delta,\vec{p},\tau) &= A_u(x)\frac{\rho_{-\tau}}{\rho_0} + A_l(x)\frac{\rho_\tau}{\rho_0} \\
&+ B(\frac{\rho}{\rho_0})^\sigma(1-x\delta^2) - 8\tau x\frac{B}{\sigma+1}\frac{\rho^{\sigma-1}}{\rho_0^\sigma}\delta\rho_{-\tau} \\
&+ \frac{2C_{\tau,\tau}}{\rho_0}\int d^3p'\frac{f_\tau(\vec{p}')}{1+(\vec{p}-\vec{p}')^2/\Lambda^2} \\
&+ \frac{2C_{\tau,-\tau}}{\rho_0}\int d^3p'\frac{f_{-\tau}(\vec{p}')}{1+(\vec{p}-\vec{p}')^2/\Lambda^2}. \qquad (1)
\end{aligned}
$$

(1) Higher E_{sym}, lower n/p ratio, lower pi^-/pi^+

(2) The E_{sym} effect shows a transition from central to peripheral reaction

(3) The E_{sym} effect is stronger at lower energies

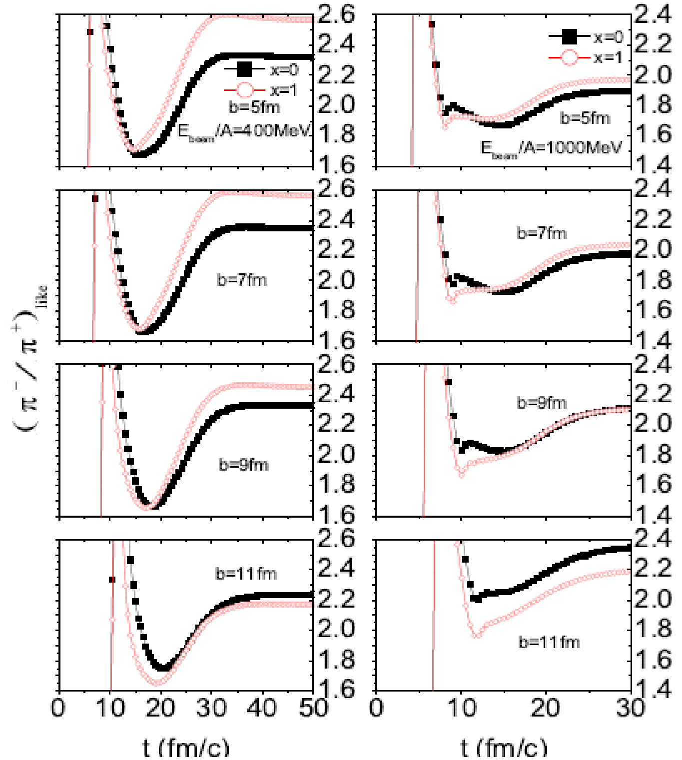

Central reaction: Mostly E_{sym} effect, little n-skin effects

400 MeV/A

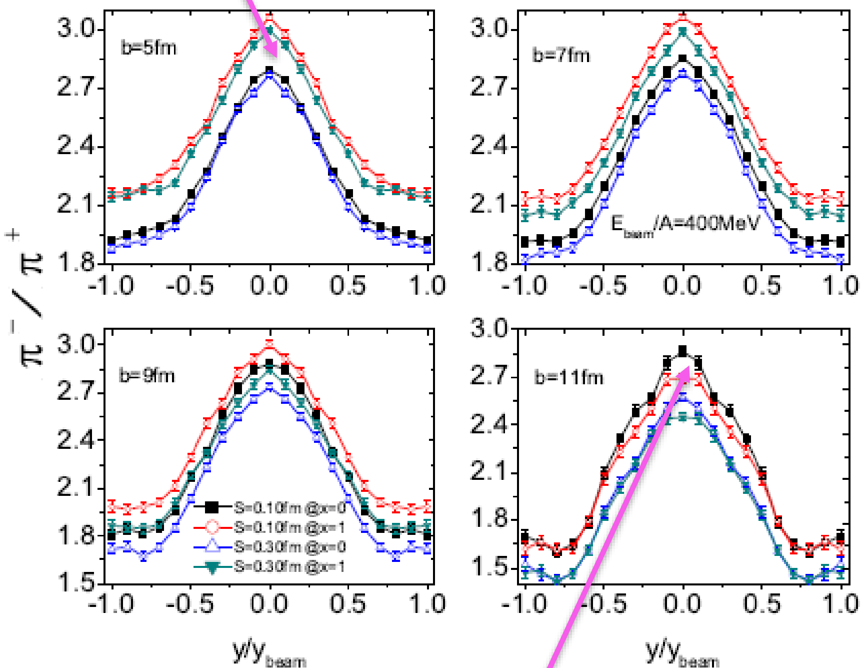

1000MeV/A

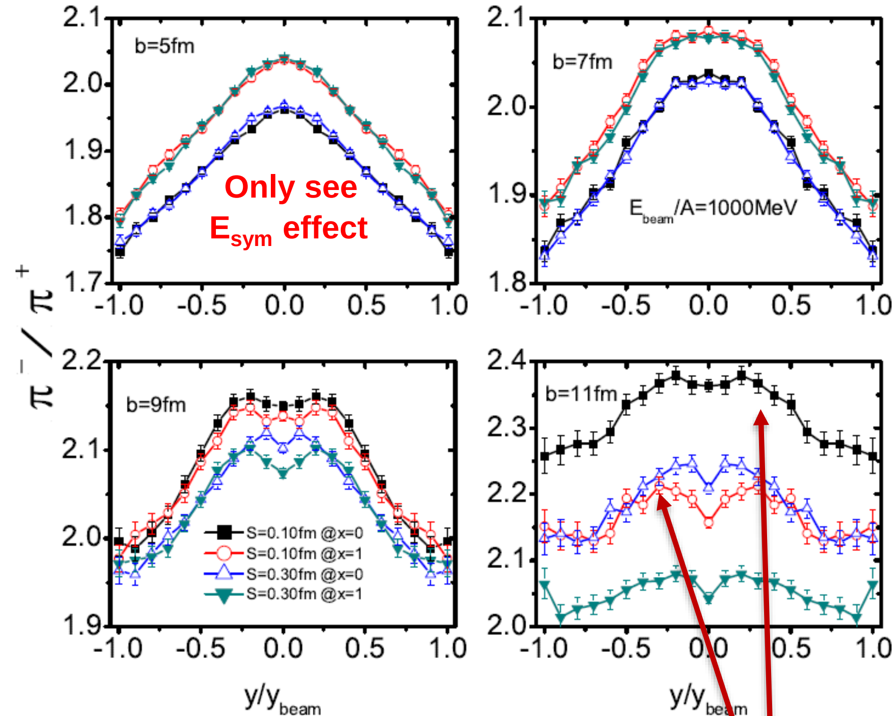

Peripheral reaction: 13% n-ski effect but 3% E_{sym} effect at mid-rapidity

n-skin & E_{sym} effects 5% compatible

E_{sym} and neutron-skin effects on observables of heavy-ion reactions

$(|y/y_{beam}| \leqslant 0.5)$

$$F(L_2) = \frac{\Delta(\pi^-/\pi^+)}{\Delta L_2/L_2}$$

L_2 is the slope of E_{sym} at $2\rho_0$

	$S = 0.10$ fm	$S = 0.30$ fm
E_{beam}(MeV)	400 (1000)	400 (1000)
$b = 5$ fm	13.7 (4.0)	12.2 (3.8)
$b = 7$ fm	11.4 (3.1)	10.4 (2.9)

$$F(S) = \frac{\Delta(\pi^-/\pi^+)}{\Delta S/S},$$

	$x = 0$	$x = 1$
E_{beam} (MeV)	400 (1000)	400 (1000)
$b = 5$ fm	4.8 (0.4)	8.9 (0.2)
$b = 7$ fm	11.0 (0.4)	13.9 (0.9)
$b = 9$ fm	22.1 (7.8)	25.2 (7.2)
$b = 11$ fm	41.8 (20.6)	33.4 (18.5)

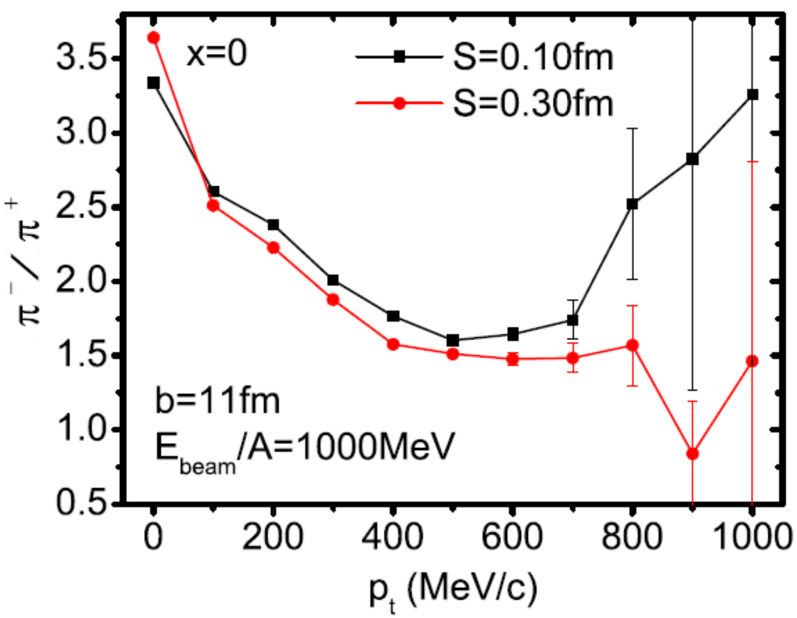

The most fundamental but lest known physics underlying the symmetry energy

Spin-isospin dependence of nucleon interactions at short distance $V_{np}(T_0) \neq V_{np}(T_1)$

EOS of dense neutron-rich matter is a major scientific driver of

(1) High-energy rare isotope beam facilities around the world

(2) Various x-ray satellites

(3) Various gravitational wave detectors

Among the promising observables sensitive to the high-density symmetry energy:

- **π^-/π^+ and n/p spectrum ratio, neutron-proton differential flow and correlation function in heavy-ion collisions at intermediate energies**
- **Neutron skins of heavy nuclei and radii of neutron stars**
- **Neutrino flux of supernova explosions**
- **Tidal polarizability in neutron star mergers, strain amplitude of gravitational waves from deformed pulsars, frequency and damping time of neutron star oscillations**

B.A. Li, L.W. Chen and C.M. Ko, Phys. Rep. 464, 113 (2008)

EPJA, Vol. 50, No. 2 (2014)

2023 White Paper:

Dense Nuclear Matter Equation of State from Heavy-Ion Collisions

Agnieszka Sorenson et al., **arXiv:2301.13253**

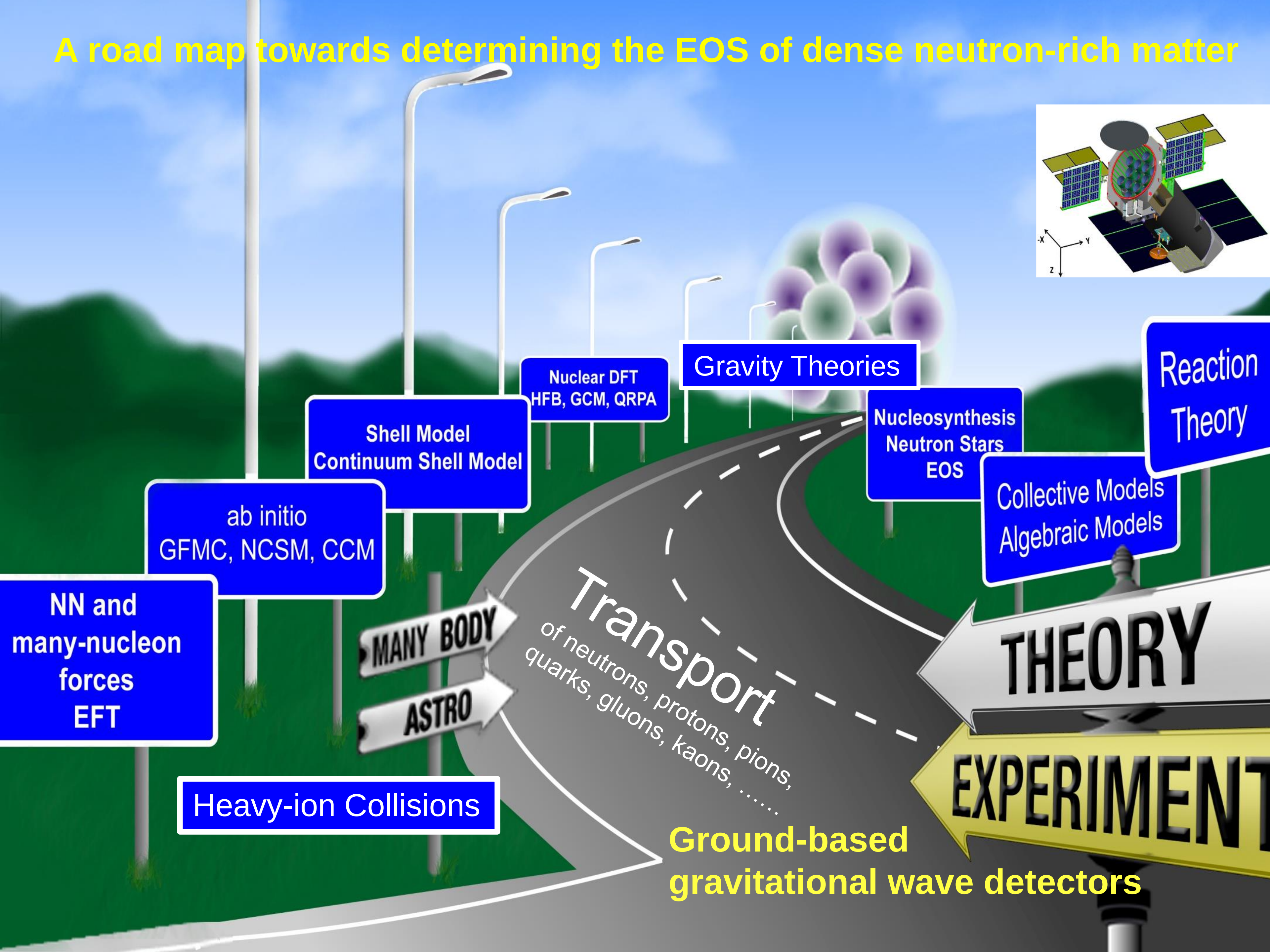
A road map towards determining the EOS of dense neutron-rich matter
Gravity Theories
Nuclear DFT
HFB, GCM, QRPA
Shell Model
Continuum Shell Model
ab initio
GFMC, NCSM, CCM
NN and
many-nucleon
forces
EFT
Nucleosynthesis
Neutron Stars
EOS
Reaction
Theory
Collective Models
Algebraic Models
MANY BODY
ASTRO
Transport
of neutrons, protons, pions,
quarks, gluons, kaons, ……
THEORY
EXPERIMENT
Heavy-ion Collisions
Ground-based
gravitational wave detectors